

Adaptive Reduced-Rank Constrained Constant Modulus Beamforming Algorithms Based on Joint Iterative Optimization of Filters

Lei Wang, Rodrigo C. de Lamare, and Masahiro Yukawa

Abstract—This paper proposes a robust reduced-rank scheme for adaptive beamforming based on joint iterative optimization (JIO) of adaptive filters. The novel scheme is designed according to the constant modulus (CM) criterion subject to different constraints, and consists of a bank of full-rank adaptive filters that forms the transformation matrix, and an adaptive reduced-rank filter that operates at the output of the bank of filters to estimate the desired signal. We describe the proposed scheme for both the direct-form processor (DFP) and the generalized sidelobe canceller (GSC) structures. For each structure, we derive stochastic gradient (SG) and recursive least squares (RLS) algorithms for its adaptive implementation. The Gram-Schmidt (GS) technique is applied to the adaptive algorithms for reformulating the transformation matrix and improving performance. An automatic rank selection technique is developed and employed to determine the most adequate rank for the derived algorithms. The complexity and convexity analyses are carried out. Simulation results show that the proposed algorithms outperform the existing full-rank and reduced-rank methods in convergence and tracking performance.

I. INTRODUCTION

Adaptive beamforming techniques have been developed to improve the reception of a desired signal while suppressing interference at the output of a sensor array. It is an ubiquitous task in array signal processing with applications in radar, sonar, astronomy, and more recently, in wireless communications [1]-[5]. A number of adaptive algorithms for the beamformer design are available and have been extensively studied [3], [4]. The most common are the linearly constrained adaptive algorithms [6]-[10]. In general, the linear constraints correspond to prior knowledge of certain parameters such as the direction of arrival (DOA) of the desired signal.

An important issue that is considered in adaptive beamforming is the design criterion. Among many adaptive algorithms found in the literature, the most promising criteria employed are the constrained minimum variance (CMV) [3] and the constrained constant modulus (CCM) [4] due to their simplicity and effectiveness. The CMV criterion aims to minimize the beamformer output power while maintaining the array response on the DOA of the desired signal. The CCM criterion is a positive measure [4] of the deviation of the beamformer output from a constant modulus condition subject to a constraint on the array response of the desired signal.

By measuring the deviation, the CCM criterion provides more information than the CMV for the parameter estimation of constant modulus constellations in the beamformer design.

Numerous adaptive algorithms have been proposed according to the constrained version criteria to realize the beamformer design [3], [6]-[11]. The major drawback of the full-rank methods, such as stochastic gradient (SG) [12] and recursive least-squares (RLS) [13], [14], is that these methods require a large amount of samples to reach the steady-state when the number of elements in the filter is large. Furthermore, in dynamic scenarios, filters with many elements usually fail or provide poor performance in tracking signals embedded in interference and noise. Reduced-rank signal processing was originally motivated to provide a way out of this dilemma [18]-[24]. For the application of beamforming, reduced-rank schemes project the received vector onto a lower dimensional subspace and perform the filter optimization within this subspace. One of the popular reduced-rank schemes is the multistage Wiener filter (MSWF), which employs the minimum mean squared error (MMSE) [26], and its extended versions that utilize the CMV and CCM criteria were reported in [27], [28]. Another technique that resembles the MSWF [29], [30] is the auxiliary-vector filtering (AVF) [31], [32]. A joint iterative optimization (JIO) scheme, which was presented recently in [37], employs the CMV criterion with a relative low-complexity adaptive implementation to achieve better performance than the existing methods.

In this paper, we introduce a robust reduced-rank scheme based on joint iterative optimization of filters with the CCM criterion in detail and compare it with that of the CMV to show its improved performance in the studied scenarios. The developed CCM reduced-rank scheme consists of a bank of full-rank adaptive filters, which constitutes the transformation matrix, and an adaptive reduced-rank filter that operates at the output of the bank of full-rank filters. The transformation matrix maps the received signal into a lower dimension, which is then processed by the reduced-rank filter to estimate the transmitted signal. The proposed scheme provides an iterative exchange of information between the transformation matrix and the reduced-rank filter and thus leads to improved convergence and tracking performance.

This paper makes two contributions:

- A reduced-rank scheme according to the constant modulus (CM) criterion subject to different constraints is proposed based on the JIO of adaptive filters. This robust reduced-rank scheme is investigated for both direct-form

Lei Wang and Rodrigo C. de Lamare are with the Department of Electronics, University of York, York, YO10 5DD, U.K. (e-mail: lw517@york.ac.uk, rcd1500@ohm.york.ac.uk).

Masahiro Yukawa is with Laboratory for Mathematical Neuroscience, BSI, RIKEN, JAPAN (e-mail:myukawa@riken.jp).

processor (DFP) and the generalized sidelobe canceller (GSC) [14] structures. For each structure, a family of computationally efficient reduced-rank SG and RLS type algorithms are derived for the proposed scheme. The Gram-Schmidt (GS) technique is employed in the proposed algorithms to reformulate the transformation matrix for further improving performance. An automatic rank selection technique is developed to determine the most adequate rank for the proposed algorithms.

- The complexity comparison is presented to show the computational costs of the proposed reduced-rank algorithms. An analysis of the convergence properties for the proposed reduced-rank scheme is carried out. Simulations are performed to show the improved convergence and tracking performance of the proposed algorithms over existing methods. The effectiveness of the GS and automatic rank selection techniques for the proposed algorithms is visible in the results.

The remainder of this paper is organized as follows: we outline a system model for beamforming in Section II. Based on this model, the full-rank and reduced-rank CCM beamformer designs are reviewed. The proposed reduced-rank scheme based on the CM criterion subject to different constraints is presented in Section III, and the proposed adaptive algorithms are detailed for implementation in Section IV. The complexity and convergence analysis of the proposed algorithms is carried out in Section V. Simulation results are provided and discussed in Section VI, and conclusions are drawn in Section VII.

II. SYSTEM MODEL AND CCM BEAMFORMER DESIGN

In this section, we first describe a system model to express the received data vector. Based on this model, the full-rank beamformer design according to the CM criterion subject to the constraint on the array response is introduced for the DFP and the GSC structures.

A. System Model

Let us suppose that q narrowband signals impinge on a uniform linear array (ULA) of m ($m \geq q$) sensor elements. The sources are assumed to be in the far field with DOAs $\theta_0, \dots, \theta_{q-1}$. The received vector $\mathbf{x}(i) \in \mathbb{C}^{m \times 1}$ at the i th snapshot can be modeled as

$$\mathbf{x}(i) = \mathbf{A}(\boldsymbol{\theta})\mathbf{s}(i) + \mathbf{n}(i), \quad i = 1, \dots, N, \quad (1)$$

where $\boldsymbol{\theta} = [\theta_0, \dots, \theta_{q-1}]^T \in \mathbb{R}^{q \times 1}$ is the signal DOAs, $\mathbf{A}(\boldsymbol{\theta}) = [\mathbf{a}(\theta_0), \dots, \mathbf{a}(\theta_{q-1})] \in \mathbb{C}^{m \times q}$ comprises the normalized signal steering vectors $\mathbf{a}(\theta_k) = [1, e^{-2\pi j \frac{u}{\lambda_c} \cos \theta_k}, \dots, e^{-2\pi j (m-1) \frac{u}{\lambda_c} \cos \theta_k}]^T \in \mathbb{C}^{m \times 1}$, ($k = 0, \dots, q-1$), where λ_c is the wavelength and u ($u = \lambda_c/2$ in general) is the inter-element distance of the ULA, and to avoid mathematical ambiguities, the steering vectors $\mathbf{a}(\theta_k)$ are assumed to be linearly independent. $\mathbf{s}(i) \in \mathbb{C}^{q \times 1}$ is the source data, $\mathbf{n}(i) \in \mathbb{C}^{m \times 1}$ is temporary white sensor noise, which is assumed to be a zero-mean spatially and Gaussian process, N is the observation size of snapshots, and $(\cdot)^T$ stands for transpose.

B. Full-rank CCM Beamformer Design

The full-rank CCM linear receiver design for beamforming is equivalent to determining a filter $\mathbf{w}(i) = [w_1(i), \dots, w_m(i)]^T \in \mathbb{C}^{m \times 1}$ that provides an estimate of the desired symbol $y(i) = \mathbf{w}^H(i)\mathbf{x}(i)$, where $(\cdot)^H$ denotes Hermitian transpose. The calculation of the weight vector is based on the minimization of the following cost function:

$$J_{\text{cm}}(\mathbf{w}(i)) = \mathbb{E}\left\{[|y(i)|^p - \nu]^2\right\}, \quad (2)$$

subject to $\mathbf{w}^H(i)\mathbf{a}(\theta_0) = \gamma$,

where ν is suitably chosen to guarantee that the weight solution is close to the global minimum and γ is set to ensure the convexity of (2) [28]. The quantity θ_0 is the direction of the desired signal, $\mathbf{a}(\theta_0)$ denotes the corresponding normalized steering vector, and in general, $p = 2$ is selected to consider the cost function as the expected deviation of the squared modulus of the beamformer output to a constant, say $\nu = 1$. The CCM criterion is a positive measure [4] of the deviation of the beamformer output from a constant modulus condition subject to a constraint on the array response of the desired signal. Compared with the CMV criterion, it exploits a constant modulus property of the transmitted signals, utilizes the deviation to provide more information for the parameter estimation of the constant modulus constellations, and achieves a superior performance [15], [28]. The CCM beamformer minimizes the contribution of interference and noise while maintaining the gain along the look direction to be constant. The weight expression of the full-rank CCM design is given in [28].

C. Reduced-rank CCM Beamformer Design

For large m , considering the high computational cost and poor performance associated with the full-rank filter, a number of recent works in the literature have been reported based on reduced-rank schemes [18]-[22], [26]-[46]. Here, we will describe a reduced-rank framework that reduces the number of coefficients by mapping the received vector into a lower dimensional subspace. The diagrams of the reduced-rank processors are depicted for the DFP and the GSC structures in Fig. 1(a) and Fig. 1(b), respectively.

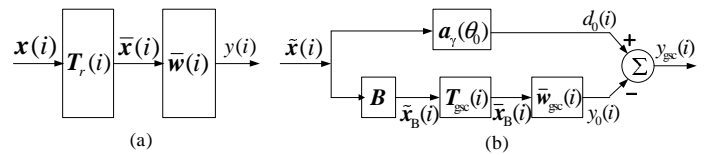


Fig. 1. Reduced-rank scheme for (a) the DFP and (b) the GSC structures.

1) *Beamformer Design for the DFP*: In the DFP structure, $\mathbf{T}_r \in \mathbb{C}^{m \times r}$ denotes the transformation matrix that includes a set of $m \times 1$ vectors for a r -dimensional subspace with $r \leq m$. The transformation matrix maps the received vector $\mathbf{x}(i)$ into its low-dimension version $\bar{\mathbf{x}}(i) \in \mathbb{C}^{r \times 1}$, which is given by

$$\bar{\mathbf{x}}(i) = \mathbf{T}_r^H(i)\mathbf{x}(i), \quad (3)$$

where, in what follows, all r -dimensional quantities are denoted by an over bar. An adaptive reduced-rank CCM filter

$\bar{\mathbf{w}}(i) \in \mathbb{C}^{r \times 1}$ follows the transformation matrix to produce the filter output $y(i) = \bar{\mathbf{w}}^H(i)\bar{\mathbf{x}}(i)$.

Substituting the expression of $y(i)$ into the cost function in (2) and calculating for the reduced-rank weight vector, we have [28]

$$\bar{\mathbf{w}}(i+1) = \bar{\mathbf{R}}^{-1}(i) \left\{ \bar{\mathbf{p}}(i) - \frac{[\bar{\mathbf{p}}^H(i)\bar{\mathbf{R}}^{-1}(i)\bar{\mathbf{a}}(\theta_0) - \gamma]\bar{\mathbf{a}}(\theta_0)}{\bar{\mathbf{a}}^H(\theta_0)\bar{\mathbf{R}}^{-1}(i)\bar{\mathbf{a}}(\theta_0)} \right\}, \quad (4)$$

where $\bar{\mathbf{R}}(i) = \mathbb{E}[|y(i)|^2 \mathbf{T}_r^H(i)\mathbf{x}(i)\mathbf{x}^H(i)\mathbf{T}_r(i)] \in \mathbb{C}^{r \times r}$, $\bar{\mathbf{a}}(\theta_0) = \mathbf{T}_r^H \mathbf{a}(\theta_0) \in \mathbb{C}^{r \times 1}$, and $\bar{\mathbf{p}}(i) = \mathbb{E}[y^*(i)\mathbf{T}_r^H(i)\mathbf{x}(i)] \in \mathbb{C}^{r \times 1}$. Note that the expression in (4) is a function of previous values of $\bar{\mathbf{w}}(i)$ (since $y(i) = \bar{\mathbf{w}}^H(i)\bar{\mathbf{x}}(i)$) and thus must be initialized to start the computation for the solution. We keep the time index in $\bar{\mathbf{R}}(i)$ and $\bar{\mathbf{p}}(i)$ for the same reason.

2) *Beamformer Design for the GSC*: The GSC structure converts the constrained optimization problem into an unconstrained one and adopts an alternative way to realize the beamformer design. The full-rank CCM beamformer design with respect to the GSC structure has been reported in [42]. Here, we employ an alternative way proposed in [47], [48] to describe a reduced-rank GSC structure. As can be seen in Fig. 1(b), the reduced-rank GSC structure composes a constrained component ($\mathbf{a}_\gamma(\theta_0) = \gamma\mathbf{a}(\theta_0)$) and an unconstrained component. $\tilde{\mathbf{x}}(i)$ is a new received vector defined as

$$\tilde{\mathbf{x}}(i) = y_{\text{gsc}}^*(i)\mathbf{x}(i), \quad (5)$$

where $y_{\text{gsc}}(i) = \mathbf{w}^H(i)\mathbf{x}(i)$. The definition of $\tilde{\mathbf{x}}(i)$ is valid for $p = 2$ in (2) and $|y_{\text{gsc}}(i)|^2 = \mathbf{w}^H(i)\tilde{\mathbf{x}}(i)$. This expression is only to favor its use in the GSC structure for the case of the CM cost function. Note that $y_{\text{gsc}}(i)$ and $y(i)$ (full-rank or reduced-rank with $\mathbf{T}_r = \mathbf{I}_{m \times m}$) correspond to the same values but are written in a different way to indicate the structures (DFP and GSC).

For the constrained component, the output is $d_0(i) = \mathbf{a}_\gamma^H(\theta_0)\tilde{\mathbf{x}}(i)$. With respect to the unconstrained component, the new received vector passes through a signal blocking matrix $\mathbf{B} \in \mathbb{C}^{(m-1) \times m}$ to get a transformed vector $\tilde{\mathbf{x}}_B(i) \in \mathbb{C}^{(m-1) \times 1}$, which is

$$\tilde{\mathbf{x}}_B(i) = \mathbf{B}\tilde{\mathbf{x}}(i), \quad (6)$$

where \mathbf{B} is obtained by the singular value decomposition or the QR decomposition algorithms [44]. Thus, $\mathbf{B}\mathbf{a}(\theta_0) = \mathbf{0}_{(m-1) \times 1}$ means that the term \mathbf{B} effectively blocks any signal coming from the look direction θ_0 . The transformation matrix $\mathbf{T}_{\text{gsc}}(i) \in \mathbb{C}^{(m-1) \times r}$ maps the transformed vector $\tilde{\mathbf{x}}_B(i)$ into a low-dimension version, as described by

$$\bar{\mathbf{x}}_B(i) = \mathbf{T}_{\text{gsc}}^H(i)\tilde{\mathbf{x}}_B(i). \quad (7)$$

The reduced-rank received vector $\bar{\mathbf{x}}_B(i)$ is processed by a reduced-rank filter $\bar{\mathbf{w}}_{\text{gsc}}(i) \in \mathbb{C}^{r \times 1}$ to get the unconstrained output $y_0(i) = \bar{\mathbf{w}}_{\text{gsc}}^H(i)\bar{\mathbf{x}}_B(i)$. The reduced-rank weight vector is [14]

$$\bar{\mathbf{w}}_{\text{gsc}}(i+1) = \bar{\mathbf{R}}_{\bar{\mathbf{x}}_B}^{-1}(i)\bar{\mathbf{p}}_B(i), \quad (8)$$

where $\bar{\mathbf{R}}_{\bar{\mathbf{x}}_B}(i) = \mathbb{E}[\mathbf{T}_{\text{gsc}}^H(i)\tilde{\mathbf{x}}_B(i)\tilde{\mathbf{x}}_B^H(i)\mathbf{T}_{\text{gsc}}(i)] \in \mathbb{C}^{r \times r}$ and $\bar{\mathbf{p}}_B(i) = \mathbb{E}[(d_0^*(i) - 1)\mathbf{T}_{\text{gsc}}^H(i)\tilde{\mathbf{x}}_B(i)] \in \mathbb{C}^{r \times 1}$. Note that this expression is a function of previous values of the weight vector

and therefore must be initialized to start the computation for the solution.

The reduced-rank GSC structure can be concluded in a transformation operator $\bar{\mathbf{S}} = [\mathbf{a}_\gamma(\theta_0), \mathbf{B}^H \mathbf{T}_{\text{gsc}}]^H \in \mathbb{C}^{(r+1)} \times m$ and a reduced-rank weight vector $\bar{\mathbf{w}}' = [1, -\bar{\mathbf{w}}_{\text{gsc}}^H]^H \in \mathbb{C}^{(r+1) \times 1}$. The equivalent full-rank weight vector can be expressed as

$$\begin{aligned} \mathbf{w}(i+1) &= \bar{\mathbf{S}}^H \bar{\mathbf{w}}'(i+1) \\ &= \mathbf{a}_\gamma(\theta_0) - \mathbf{B}^H \mathbf{T}_{\text{gsc}}(i+1)\bar{\mathbf{w}}_{\text{gsc}}(i+1). \end{aligned} \quad (9)$$

The reduced-rank weight expressions in (4) for the DFP and in (9) for the GSC are general forms to the signal processing tasks. Specifically, for $r = m$ (DFP) and $r = m-1$ (GSC), the expressions are equivalent to the full-rank filtering schemes [14]. For $1 < r < m$ (DFP) and $1 < r < m-1$ (GSC), the signal processing tasks are changed and the reduced-rank filters estimate the desired signals.

The challenge left to us is how to efficiently design and calculate the transformation matrices \mathbf{T}_r and \mathbf{T}_{gsc} . The principal components (PC) method reported in [18] uses the eigenvectors of the interference-only covariance matrix corresponding to the eigenvalues of significant magnitude to construct the transformation matrix. The cross-spectral (CS) method [21], a counterpart of the PC method belonging to the eigen-decomposition family, forms the transformation matrix by using the eigenvectors which contribute the most towards maximizing the SINR and outperforms the PC method. Another family of adaptive reduced-rank filters such as the MSWF [26], [27] and the AVF [31] generates a set of basis vectors as the transformation matrix that spans the same Krylov subspace [29], [30].

III. PROPOSED CCM REDUCED-RANK SCHEME

In this section, we introduce the proposed reduced-rank scheme based on the JIO approach. Two optimization problems according to the CM criterion subject to different constraints are described for the proposed scheme. Based on this scheme, we derive the expressions of the transformation matrix and the reduced-rank weight vector. For the sake of completeness, the proposed scheme is realized for both the DFP and the GSC structures.

A. Proposed CCM Reduced-rank Scheme for the DFP

Here we detail the principles of the proposed CCM reduced-rank scheme using a transformation based on adaptive filters. For the DFP structure depicted in Fig. 2(a), the proposed scheme employs a transformation matrix $\mathbf{T}_r(i) \in \mathbb{C}^{m \times r}$, which is responsible for the dimensionality reduction, to generate $\bar{\mathbf{x}}(i) \in \mathbb{C}^{r \times 1}$. The dimension is reduced and the key features of the original signal is retained in $\bar{\mathbf{x}}(i)$ according to the CCM criterion. The transformation matrix is structured as a bank of r full-rank filters $\mathbf{t}_j(i) = [t_{1,j}(i), t_{2,j}(i), \dots, t_{m,j}(i)]^T \in \mathbb{C}^{m \times 1}$, ($j = 1, \dots, r$) as given by $\mathbf{T}_r(i) = [\mathbf{t}_1(i), \mathbf{t}_2(i), \dots, \mathbf{t}_r(i)]$. An adaptive reduced-rank filter $\bar{\mathbf{w}}(i) \in \mathbb{C}^{r \times 1}$ is then used to produce the output. The transformation matrix $\mathbf{T}_r(i)$ and the reduced-rank filter $\bar{\mathbf{w}}(i)$ are jointly optimized in the proposed scheme.

The filter output is a function of the received vector, the transformation matrix, and the reduced-rank weight vector, which is

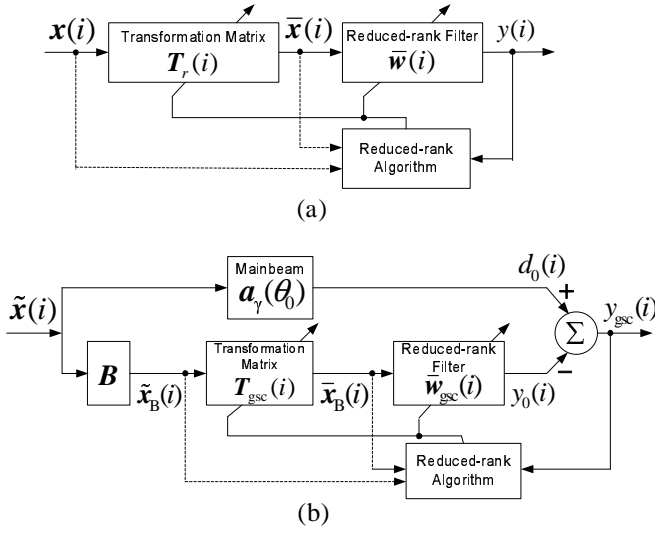


Fig. 2. Proposed reduced-rank scheme for (a) the DFP and (b) the GSC structures.

$$y(i) = \bar{\mathbf{w}}^H(i) \mathbf{T}_r^H(i) \mathbf{x}(i) = \bar{\mathbf{w}}^H(i) \bar{\mathbf{x}}(i). \quad (10)$$

We describe two optimization problems according to the CM cost function subject to different constraints for the proposed reduced-rank scheme, which are given by

$$\begin{aligned} \text{Problem 1: } \min J_{\text{cm}}(\mathbf{T}_r(i), \bar{\mathbf{w}}(i)) &= \mathbb{E} \left\{ [|y(i)|^2 - 1]^2 \right\} \\ \text{subject to } \bar{\mathbf{w}}^H(i) \mathbf{T}_r^H(i) \mathbf{a}(\theta_0) &= \gamma, \end{aligned} \quad (11)$$

$$\begin{aligned} \text{Problem 2: } \min J_{\text{cm}}(\mathbf{T}_r(i), \bar{\mathbf{w}}(i)) &= \mathbb{E} \left\{ [|y(i)|^2 - 1]^2 \right\} \\ \text{subject to } \bar{\mathbf{w}}^H(i) \mathbf{T}_r^H(i) \mathbf{a}(\theta_0) &= \gamma \text{ and } \mathbf{T}_r^H(i) \mathbf{T}_r(i) = \mathbf{I}. \end{aligned} \quad (12)$$

Compared with (11), the problem in (12) has an orthogonal constraint on the transformation matrix, which is to reformulate $\mathbf{T}_r(i)$. The transformation matrix generated from (11) has vectors that may perform a similar operation (e.g., take the same information twice or more), thereby making poor use of the data and losing performance. The subspace computed with (12), which spans the same subspace as $\mathbf{T}_r(i)$, generates basis vectors that are orthogonal to each other and which does not affect the noise statistically. The reformulated transformation matrix performs an efficient operation to keep all useful information in the generated reduced-rank received vector, which is important to estimate the desired signal and improve the performance. In the following, we will derive the CCM expressions of $\mathbf{T}_r(i)$ and $\bar{\mathbf{w}}(i)$ for solving (11) and (12).

The cost function in (11) can be transformed by the method of Lagrange multipliers into an unconstrained one, which is

$$\begin{aligned} L_{\text{cm}}(\mathbf{T}_r(i), \bar{\mathbf{w}}(i)) &= \mathbb{E} \left\{ [|\bar{\mathbf{w}}^H(i) \mathbf{T}_r^H(i) \mathbf{x}(i)|^2 - 1]^2 \right\} \\ &+ 2\Re \left\{ \lambda [\bar{\mathbf{w}}^H(i) \mathbf{T}_r^H(i) \mathbf{a}(\theta_0) - \gamma] \right\}, \end{aligned} \quad (13)$$

where λ is a scalar Lagrange multiplier and the operator $\Re(\cdot)$ selects the real part of the argument.

Assuming $\bar{\mathbf{w}}(i)$ is known, computing the gradient of (13) with respect to $\mathbf{T}_r(i)$ (matrix calculus), equating it to a null matrix and solving for λ , we have

$$\begin{aligned} \mathbf{T}_r(i+1) &= \mathbf{R}^{-1}(i) \left\{ \mathbf{p}(i) \bar{\mathbf{w}}^H(i) - \right. \\ &\left. \frac{[\bar{\mathbf{w}}^H(i) \bar{\mathbf{R}}_{\bar{\mathbf{w}}}^{-1}(i) \bar{\mathbf{w}}(i) \mathbf{p}^H(i) \mathbf{R}^{-1}(i) \mathbf{a}(\theta_0) - \gamma] \mathbf{a}(\theta_0) \bar{\mathbf{w}}^H(i)}{\bar{\mathbf{w}}^H(i) \bar{\mathbf{R}}_{\bar{\mathbf{w}}}^{-1}(i) \bar{\mathbf{w}}(i) \mathbf{a}^H(\theta_0) \mathbf{R}^{-1}(i) \mathbf{a}(\theta_0)} \right\} \bar{\mathbf{R}}_{\bar{\mathbf{w}}}^{-1}(i), \end{aligned} \quad (14)$$

where $\mathbf{p}(i) = \mathbb{E}[y^*(i) \mathbf{x}(i)] \in \mathbb{C}^{m \times 1}$, $\mathbf{R}(i) = \mathbb{E}[|y(i)|^2 \mathbf{x}(i) \mathbf{x}^H(i)] \in \mathbb{C}^{m \times m}$, and $\bar{\mathbf{R}}_{\bar{\mathbf{w}}}(i) = \mathbb{E}[\bar{\mathbf{w}}(i) \bar{\mathbf{w}}^H(i)] \in \mathbb{C}^{r \times r}$. Note that the reduced-rank weight vector $\bar{\mathbf{w}}(i)$ depends on the received vectors that are random in practice, thus $\bar{\mathbf{R}}_{\bar{\mathbf{w}}}(i)$ is r -rank and invertible. $\mathbf{R}(i)$ and $\mathbf{p}(i)$ are functions of previous values of $\mathbf{T}_r(i)$ and $\bar{\mathbf{w}}(i)$ due to the presence of $y(i)$. Therefore, it is necessary to initialize $\mathbf{T}_r(i)$ and $\bar{\mathbf{w}}(i)$ to estimate $\mathbf{R}(i)$ and $\mathbf{p}(i)$, and start the computation.

On the other hand, assuming $\mathbf{T}_r(i)$ is known, computing the gradient of (13) with respect to $\bar{\mathbf{w}}(i)$, equating it to a null vector, and solving for λ , we obtain

$$\bar{\mathbf{w}}(i+1) = \bar{\mathbf{R}}^{-1}(i) \left\{ \bar{\mathbf{p}}(i) - \frac{[\bar{\mathbf{p}}^H(i) \bar{\mathbf{R}}^{-1}(i) \bar{\mathbf{a}}(\theta_0) - \gamma] \bar{\mathbf{a}}(\theta_0)}{\bar{\mathbf{a}}^H(\theta_0) \bar{\mathbf{R}}^{-1}(i) \bar{\mathbf{a}}(\theta_0)} \right\}, \quad (15)$$

where $\bar{\mathbf{R}}(i) = \mathbb{E}[|y(i)|^2 \mathbf{T}_r^H(i) \mathbf{x}(i) \mathbf{x}^H(i) \mathbf{T}_r(i)] \in \mathbb{C}^{r \times r}$, $\bar{\mathbf{p}}(i) = \mathbb{E}[y^*(i) \mathbf{T}_r^H(i) \mathbf{x}(i)] \in \mathbb{C}^{r \times 1}$, and $\bar{\mathbf{a}}(\theta_0) = \mathbf{T}_r^H(i) \mathbf{a}(\theta_0)$.

Note that the expressions in (14) for the transformation matrix and (15) for the reduced-rank weight vector can be applied to solve the optimization problem (12). The orthogonal constraint in (12) can be realized by the Gram-Schmidt (GS) technique, which will be illustrated in the next section.

B. Proposed CCM Reduced-rank Scheme for the GSC

For the GSC structure, as depicted in Fig. 2(b), the proposed scheme utilizes a transformation matrix $\mathbf{T}_{\text{gsc}}(i) \in \mathbb{C}^{(m-1) \times r}$ to map the new transformed vector $\tilde{\mathbf{x}}_B(i) \in \mathbb{C}^{(m-1) \times 1}$ into a lower dimension, say $\bar{\mathbf{x}}_B(i) = \mathbf{T}_{\text{gsc}}^H(i) \tilde{\mathbf{x}}_B(i) \in \mathbb{C}^{r \times 1}$. In our design, the transformation matrix $\mathbf{T}_{\text{gsc}}(i)$ and the reduced-rank weight vector $\bar{\mathbf{w}}_{\text{gsc}}(i)$ for the sidelobe of the GSC are jointly optimized by minimizing the cost function

$$\begin{aligned} J_{\text{cm-gsc}}(\mathbf{T}_{\text{gsc}}(i), \bar{\mathbf{w}}_{\text{gsc}}(i)) &= \\ &\mathbb{E} \left\{ [(\mathbf{a}_\gamma(\theta_0) - \mathbf{B}^H \mathbf{T}_{\text{gsc}}(i) \bar{\mathbf{w}}_{\text{gsc}}(i))^H \tilde{\mathbf{x}}(i) - 1]^2 \right\}, \end{aligned} \quad (16)$$

where the expression in (16) for the GSC is obtained by substituting (5) and (9) into (2) with $p = 2$. This is an unconstrained cost function that corresponds to (11). From Fig. 2 (b), this structure essentially decomposes the adaptive weight vector into constrained (array response) and unconstrained components (see also Eq. (9)). The unconstrained component can be adjusted to meet the CM criterion since the constrained component always ensures that the constrained condition is

satisfied. Thus, the proposed GSC framework converts the constrained optimization problem into an unconstrained one.

Assuming $\bar{\mathbf{w}}_{\text{gsc}}(i)$ and $\mathbf{T}_{\text{gsc}}(i)$ are given, respectively, computing the gradient of (16) with respect to $\mathbf{T}_{\text{gsc}}(i)$ and $\bar{\mathbf{w}}_{\text{gsc}}(i)$, and solving the equations yields

$$\mathbf{T}_{\text{gsc}}(i+1) = \mathbf{R}_{\tilde{\mathbf{x}}_B}^{-1}(i) \tilde{\mathbf{p}}_B(i) \bar{\mathbf{w}}_{\text{gsc}}^H(i) \bar{\mathbf{R}}_{\bar{\mathbf{w}}_{\text{gsc}}}^{-1}(i), \quad (17)$$

$$\bar{\mathbf{w}}_{\text{gsc}}(i+1) = \bar{\mathbf{R}}_{\tilde{\mathbf{x}}_B}^{-1}(i) \tilde{\mathbf{p}}_B(i), \quad (18)$$

where $\mathbf{R}_{\tilde{\mathbf{x}}_B}(i)$ and $\tilde{\mathbf{p}}_B(i)$ have been defined in the previous section, and $\bar{\mathbf{R}}_{\bar{\mathbf{w}}_{\text{gsc}}}(i) = \mathbb{E}[\bar{\mathbf{w}}_{\text{gsc}}(i) \bar{\mathbf{w}}_{\text{gsc}}^H(i)] \in \mathbb{C}^{r \times r}$. $\bar{\mathbf{R}}_{\bar{\mathbf{w}}_{\text{gsc}}}(i)$ is invertible since $\bar{\mathbf{w}}_{\text{gsc}}(i)$ depends on the random received vector and $\bar{\mathbf{R}}_{\bar{\mathbf{w}}_{\text{gsc}}}(i)$ is a full-rank matrix. $\bar{\mathbf{R}}_{\tilde{\mathbf{x}}_B}(i) = \mathbb{E}[\mathbf{T}_{\text{gsc}}^H(i) \tilde{\mathbf{x}}_B(i) \tilde{\mathbf{x}}_B^H(i) \mathbf{T}_{\text{gsc}}(i)] \in \mathbb{C}^{r \times r}$ and $\tilde{\mathbf{p}}_B(i) = \mathbb{E}[(d_0^*(i) - 1) \mathbf{T}_{\text{gsc}}^H(i) \tilde{\mathbf{x}}_B(i)] \in \mathbb{C}^{r \times 1}$. Again, the orthogonal constraint on the transformation matrix can be enforced in the optimization problem (16) and the GS technique is employed to realize this.

Note that the filter expressions in (14) and (15) for the DFP and (17) and (18) for the GSC are not closed-form solutions. In the DFP structure, the expression of the transformation matrix in (14) is a function of $\bar{\mathbf{w}}(i)$ and the reduced-rank weight vector obtained from (15) depends on $\mathbf{T}_r(i)$. It is necessary to set initial values of $\mathbf{T}_r(i)$ and $\bar{\mathbf{w}}(i)$ for the update procedures. Thus, initialization about the transformation matrix and the reduced-rank weight vector is not only to get a beamformer output $y(i)$ for estimating $\mathbf{R}(i)$ and $\bar{\mathbf{R}}(i)$, but to start the computation of the proposed scheme. In the case of the GSC, we initialize $\mathbf{T}_{\text{gsc}}(i)$ and $\bar{\mathbf{w}}_{\text{gsc}}(i)$ with the same intention.

Unlike the MSWF [26] and the AVF [31] techniques in which the transformation matrix is computed independently from the reduced-rank filter, the proposed scheme provides an iterative exchange of information between the transformation matrix and the reduced-rank filter, which leads to improved convergence and tracking performance. The transformation matrix reduces the dimension of the received vector whereas the reduced-rank filter attempts to estimate the desired signal. The key strategy lies in the joint iterative optimization of the filters. In the next section, we will derive iterative solutions via simple adaptive algorithms and introduce an automatic rank selection technique for the adaptation of the rank r .

IV. ADAPTIVE ALGORITHMS OF THE PROPOSED CCM REDUCED-RANK SCHEME

We derive SG and RLS type algorithms for the proposed CCM reduced-rank scheme. Some related works can be found in [11]-[13]. In this paper, the adaptive algorithms are described for the DFP and the GSC structures, respectively, to perform joint iterative updates of the transformation matrix and the reduced-rank weight vector. They are used to solve Problem 1. The Gram-Schmidt (GS) technique is employed in these algorithms and imposes an orthogonal constraint on the transformation matrix to solve Problem 2. An automatic rank selection technique is introduced to determine the most adequate rank for the proposed methods.

TABLE I
THE JIO-CCM-SG ALGORITHM FOR DFP

Initialization:
$\mathbf{T}_r(1) = [\mathbf{I}_{r \times r} \ \mathbf{0}_{r \times (m-r)}]^T$;
$\bar{\mathbf{w}}(1) = \mathbf{T}_r^H(1) \mathbf{a}_\gamma(\theta_0) / (\ \mathbf{T}_r^H(1) \mathbf{a}_\gamma(\theta_0)\ ^2)$.
Update for each time instant i
$y(i) = \bar{\mathbf{w}}^H(i) \mathbf{T}_r^H(i) \mathbf{x}(i)$; $e(i) = y(i) ^2 - 1$
$\mathbf{T}_r(i+1) = \mathbf{T}_r(i) - \mu_{T_r} e(i) \mathbf{y}^*(i) [\mathbf{I} - \mathbf{a}(\theta_0) \mathbf{a}^H(\theta_0)] \mathbf{x}(i) \bar{\mathbf{w}}^H(i)$
$y(i) = \bar{\mathbf{w}}^H(i) \mathbf{T}_r^H(i+1) \mathbf{x}(i)$; $e(i) = y(i) ^2 - 1$
$\bar{\mathbf{a}}(\theta_0) = \mathbf{T}_r^H(i+1) \mathbf{a}(\theta_0)$, $\tilde{\mathbf{x}}(i) = \mathbf{T}_r^H(i+1) \mathbf{x}(i)$
$\bar{\mathbf{w}}(i+1) = \bar{\mathbf{w}}(i) - \mu_{\bar{\mathbf{w}}} e(i) \mathbf{y}^*(i) [\mathbf{I} - \frac{\bar{\mathbf{a}}(\theta_0) \bar{\mathbf{a}}^H(\theta_0)}{\bar{\mathbf{a}}^H(\theta_0) \bar{\mathbf{a}}(\theta_0)}] \tilde{\mathbf{x}}(i)$

A. Stochastic Gradient Algorithms

Here, we derive the SG algorithms with the proposed CCM reduced-rank scheme for both the DFP and the GSC structures.

1) *SG algorithm for the DFP*: Assuming $\bar{\mathbf{w}}(i)$ and $\mathbf{T}_r(i)$ are known, respectively, computing the instantaneous gradient of (13) with respect to $\mathbf{T}_r(i)$ and $\bar{\mathbf{w}}(i)$, we obtain

$$\nabla L_{\text{cm}_{T_r(i)}}(i) = 2e(i) \mathbf{y}^*(i) \mathbf{x}(i) \bar{\mathbf{w}}^H(i) + 2\lambda_{T_r}^* \mathbf{a}(\theta_0) \bar{\mathbf{w}}^H(i), \quad (19)$$

$$\nabla L_{\text{cm}_{\bar{\mathbf{w}}(i)}}(i) = 2e(i) \mathbf{y}^*(i) \mathbf{T}_r^H(i) \mathbf{x}(i) + 2\lambda_{\bar{\mathbf{w}}}^* \mathbf{T}_r^H(i) \mathbf{a}(\theta_0), \quad (20)$$

where $e(i) = |y(i)|^2 - 1$.

Following the gradient rules $\mathbf{T}_r(i+1) = \mathbf{T}_r(i) - \mu_{T_r} \nabla J_{\text{un}_{T_r(i)}}(i)$ and $\bar{\mathbf{w}}(i+1) = \bar{\mathbf{w}}(i) - \mu_{\bar{\mathbf{w}}} \nabla J_{\text{un}_{\bar{\mathbf{w}}(i)}}(i)$, substituting (19) and (20) into them, respectively, and solving the Lagrange multipliers λ_{T_r} and $\lambda_{\bar{\mathbf{w}}}$ by employing the constraint in (11), we obtain the iterative SG algorithm for the DFP, which is denominated as JIO-CCM-SG. A summary of this algorithm is given in Table I, where μ_{T_r} and $\mu_{\bar{\mathbf{w}}}$ are the corresponding step size factors for the DFP, which are small positive values. The initialization values are set to satisfy the constraint in (11). The transformation matrix $\mathbf{T}_r(i)$ and the reduced-rank weight vector $\bar{\mathbf{w}}(i)$ operate together and exchange information at each time instant.

2) *SG algorithm for the GSC*: For the GSC structure, assuming $\bar{\mathbf{w}}_{\text{gsc}}(i)$ and $\mathbf{T}_{\text{gsc}}(i)$ are given in (16), respectively, we get

$$\nabla J_{\text{cm-gsc}_{T_{\text{gsc}}(i)}}(i) = e_{\text{gsc}}^*(i) \tilde{\mathbf{x}}_B(i) \bar{\mathbf{w}}_{\text{gsc}}^H(i), \quad (21)$$

$$\nabla J_{\text{cm-gsc}_{\bar{\mathbf{w}}_{\text{gsc}}(i)}}(i) = e_{\text{gsc}}^*(i) \tilde{\mathbf{x}}_B(i), \quad (22)$$

where $e_{\text{gsc}}(i) = 1 - \mathbf{w}^H(i) \tilde{\mathbf{x}}(i)$ and $\mathbf{w}(i)$ is obtained from (9).

Substituting (21) and (22) into the gradient rules, we obtain the iterative SG algorithm for the GSC, which is summarized in Table II. where $\mu_{T_{\text{gsc}}}$ and $\mu_{\bar{\mathbf{w}}_{\text{gsc}}}$ are the corresponding step size factors for the GSC.

B. Recursive Least Squares Algorithms

In this part, we derive the RLS algorithms with the proposed CCM reduced-rank scheme for both the DFP and the GSC structures.

TABLE II
THE JIO-CCM-SG ALGORITHM FOR GSC

Initialization:
 $\mathbf{T}_{\text{gsc}}(1) = [\mathbf{I}_{r \times r} \ \mathbf{0}_{r \times (m-r)}]^T$; $\bar{\mathbf{w}}_{\text{gsc}}(1) = \mathbf{I}_{r \times 1}$.
Update for each time instant i
 $\mathbf{w}(i) = \mathbf{a}_\gamma(\theta_0) - \mathbf{B}^H \mathbf{T}_{\text{gsc}}(i) \bar{\mathbf{w}}_{\text{gsc}}(i)$, $y_{\text{gsc}}(i) = \mathbf{w}^H(i) \mathbf{x}(i)$
 $\tilde{\mathbf{x}}(i) = y_{\text{gsc}}^*(i) \mathbf{x}(i)$, $\tilde{\mathbf{x}}_B(i) = \mathbf{B} \tilde{\mathbf{x}}(i)$, $e_{\text{gsc}}(i) = 1 - \mathbf{w}^H(i) \tilde{\mathbf{x}}(i)$
 $\mathbf{T}_{\text{gsc}}(i+1) = \mathbf{T}_{\text{gsc}}(i) - \mu_{T_r} e_{\text{gsc}}^*(i) \tilde{\mathbf{x}}_B(i) \bar{\mathbf{w}}_{\text{gsc}}^H(i)$
 $\mathbf{w}(i) = \mathbf{a}_\gamma(\theta_0) - \mathbf{B}^H \mathbf{T}_{\text{gsc}}(i+1) \bar{\mathbf{w}}_{\text{gsc}}(i)$
 $y_{\text{gsc}}(i) = \mathbf{w}^H(i) \mathbf{x}(i)$, $\tilde{\mathbf{x}}(i) = y_{\text{gsc}}^*(i) \mathbf{x}(i)$, $\tilde{\mathbf{x}}_B(i) = \mathbf{B} \tilde{\mathbf{x}}(i)$
 $e_{\text{gsc}}(i) = 1 - \mathbf{w}^H(i) \tilde{\mathbf{x}}(i)$, $\tilde{\mathbf{x}}_B(i) = \mathbf{T}_{\text{gsc}}^H(i+1) \tilde{\mathbf{x}}_B(i)$
 $\bar{\mathbf{w}}_{\text{gsc}}(i+1) = \bar{\mathbf{w}}_{\text{gsc}}(i) - \mu_{\bar{\mathbf{w}}_{\text{gsc}}} e_{\text{gsc}}^*(i) \tilde{\mathbf{x}}_B(i)$

1) *RLS algorithm for the DFP*: Considering the DFP case, the unconstrained least squares (LS) cost function is given by

$$L_{\text{un}}(\mathbf{T}_r(i), \bar{\mathbf{w}}(i)) = \sum_{l=1}^i \alpha^{i-l} [|\bar{\mathbf{w}}^H(i) \mathbf{T}_r^H(i) \mathbf{x}(l)|^2 - 1]^2 + 2\Re \left\{ \lambda [\bar{\mathbf{w}}^H(i) \mathbf{T}_r^H(i) \mathbf{a}(\theta_0) - \gamma] \right\}, \quad (23)$$

where α is a forgetting factor chosen as a positive constant close to, but less than 1.

Assuming $\bar{\mathbf{w}}(i)$ and $\mathbf{T}_r(i)$ are known in (23), respectively, we obtain

$$\mathbf{T}_r(i+1) = \hat{\mathbf{R}}^{-1}(i) \left\{ \hat{\mathbf{p}}(i) - \frac{[\hat{\mathbf{p}}^H(i) \hat{\mathbf{R}}^{-1}(i) \mathbf{a}(\theta_0) - \gamma] \mathbf{a}(\theta_0)}{\mathbf{a}^H(\theta_0) \hat{\mathbf{R}}^{-1}(i) \mathbf{a}(\theta_0)} \right\} \frac{\bar{\mathbf{w}}^H(i)}{\|\bar{\mathbf{w}}(i)\|^2}, \quad (24)$$

$$\bar{\mathbf{w}}(i+1) = \hat{\mathbf{R}}^{-1}(i) \left\{ \hat{\mathbf{p}}(i) - \frac{[\hat{\mathbf{p}}^H(i) \hat{\mathbf{R}}^{-1}(i) \bar{\mathbf{a}}(\theta_0) - \gamma] \bar{\mathbf{a}}(\theta_0)}{\bar{\mathbf{a}}^H(i) \hat{\mathbf{R}}^{-1}(i) \bar{\mathbf{a}}(\theta_0)} \right\}, \quad (25)$$

where $\hat{\mathbf{R}}(i) = \sum_{l=1}^i \alpha^{i-l} |y(l)|^2 \mathbf{x}(l) \mathbf{x}^H(l)$, $\hat{\mathbf{R}}(i) = \sum_{l=1}^i \alpha^{i-l} |y(l)|^2 \tilde{\mathbf{x}}(l) \tilde{\mathbf{x}}^H(l)$, $\hat{\mathbf{p}}(i) = \sum_{l=1}^i \alpha^{i-l} y^*(l) \mathbf{x}(l)$, and $\hat{\mathbf{p}}(i) = \sum_{l=1}^i \alpha^{i-l} y^*(l) \tilde{\mathbf{x}}(l)$ with $y(i)$ expressed in (10). The derivation of (24) is given in the appendix. Note that $\hat{\mathbf{R}}(i)$ is not invertible if $i < m$. It can be implemented by employing the diagonal loading technique [3], [4]. This same procedure is also used for the remaining matrices.

To avoid the matrix inversion and reduce the complexity, we employ the matrix inversion lemma [14] to update $\hat{\mathbf{R}}^{-1}(i)$ and $\hat{\mathbf{R}}(i)$ iteratively. The resulting adaptive algorithm, which we denominate as JIO-CCM-RLS, is summarized in Table III, where $\hat{\mathbf{\Phi}}(i) = \hat{\mathbf{R}}^{-1}(i)$ and $\hat{\mathbf{\Phi}}(i) = \hat{\mathbf{R}}^{-1}(i)$ are defined for concise presentation, $\mathbf{k}(i) \in \mathbb{C}^{m \times 1}$ and $\bar{\mathbf{k}}(i) \in \mathbb{C}^{r \times 1}$ are the full-rank and reduced-rank gain vectors, respectively. The recursive procedures are implemented by initializing $\hat{\mathbf{\Phi}}(0) = \delta \mathbf{I}_{m \times m}$ and $\hat{\mathbf{\Phi}}(0) = \bar{\delta} \mathbf{I}_{r \times r}$, where δ and $\bar{\delta}$ are positive scalars.

TABLE III
THE JIO-CCM-RLS ALGORITHM FOR DFP

Initialization:
 $\mathbf{T}_r(1) = [\mathbf{I}_{r \times r} \ \mathbf{0}_{r \times (m-r)}]^T$;
 $\bar{\mathbf{w}}(1) = \mathbf{T}_r^H(1) \mathbf{a}_\gamma(\theta_0) / (\|\mathbf{T}_r^H(1) \mathbf{a}_\gamma(\theta_0)\|^2)$;
 $\hat{\mathbf{\Phi}}(0) = \delta \mathbf{I}_{m \times m}$, $\hat{\mathbf{\Phi}}(0) = \bar{\delta} \mathbf{I}_{r \times r}$, $\hat{\mathbf{p}}(0) = \mathbf{0}_{m \times 1}$, $\hat{\mathbf{p}}(0) = \mathbf{0}_{r \times 1}$.
Update for each time instant i
 $y(i) = \bar{\mathbf{w}}^H(i) \mathbf{T}_r^H(i) \mathbf{x}(i)$, $\hat{\mathbf{p}}(i) = \alpha \hat{\mathbf{p}}(i-1) + y^*(i) \mathbf{x}(i)$
 $\mathbf{k}(i) = \frac{\alpha^{-1} \hat{\mathbf{\Phi}}(i-1) \mathbf{x}(i)}{(1/|y(i)|^2) + \alpha^{-1} \mathbf{x}^H(i) \hat{\mathbf{\Phi}}(i-1) \mathbf{x}(i)}$
 $\hat{\mathbf{\Phi}}(i) = \alpha^{-1} \hat{\mathbf{\Phi}}(i-1) - \alpha^{-1} \mathbf{k}(i) \mathbf{x}^H(i) \hat{\mathbf{\Phi}}(i-1)$
 $\mathbf{T}_r(i+1) = \hat{\mathbf{\Phi}}(i) \left\{ \hat{\mathbf{p}}(i) - \frac{[\hat{\mathbf{p}}^H(i) \hat{\mathbf{\Phi}}(i) \mathbf{a}(\theta_0) - \gamma] \mathbf{a}(\theta_0)}{\mathbf{a}^H(\theta_0) \hat{\mathbf{\Phi}}(i) \mathbf{a}(\theta_0)} \right\} \frac{\bar{\mathbf{w}}^H(i)}{\|\bar{\mathbf{w}}(i)\|^2}$
 $y(i) = \bar{\mathbf{w}}^H(i) \mathbf{T}_r^H(i+1) \mathbf{x}(i)$, $\bar{\mathbf{a}}(\theta_0) = \mathbf{T}_r^H(i+1) \mathbf{a}(\theta_0)$
 $\tilde{\mathbf{x}}(i) = \mathbf{T}_r^H(i+1) \mathbf{x}(i)$, $\hat{\mathbf{p}}(i) = \alpha \hat{\mathbf{p}}(i-1) + y^*(i) \tilde{\mathbf{x}}(i)$
 $\bar{\mathbf{k}}(i) = \frac{\alpha^{-1} \hat{\mathbf{\Phi}}(i-1) \tilde{\mathbf{x}}(i)}{(1/|y(i)|^2) + \alpha^{-1} \tilde{\mathbf{x}}^H(i) \hat{\mathbf{\Phi}}(i-1) \tilde{\mathbf{x}}(i)}$
 $\hat{\mathbf{\Phi}}(i) = \alpha^{-1} \hat{\mathbf{\Phi}}(i-1) - \alpha^{-1} \bar{\mathbf{k}}(i) \tilde{\mathbf{x}}^H(i) \hat{\mathbf{\Phi}}(i-1)$
 $\bar{\mathbf{w}}(i+1) = \hat{\mathbf{\Phi}}(i) \left\{ \hat{\mathbf{p}}(i) - \frac{[\hat{\mathbf{p}}^H(i) \hat{\mathbf{\Phi}}(i) \bar{\mathbf{a}}(\theta_0) - \gamma] \bar{\mathbf{a}}(\theta_0)}{\bar{\mathbf{a}}^H(i) \hat{\mathbf{\Phi}}(i) \bar{\mathbf{a}}(\theta_0)} \right\}$

2) *RLS algorithm for the GSC*: For the GSC structure, the LS cost function is given by

$$L_{\text{un-gsc}}(\mathbf{T}_{\text{gsc}}(i), \bar{\mathbf{w}}_{\text{gsc}}(i)) = \sum_{l=1}^i \alpha^{i-l} \left\{ [\mathbf{a}_\gamma(\theta_0) - \mathbf{B}^H \mathbf{T}_{\text{gsc}}(i) \bar{\mathbf{w}}_{\text{gsc}}(i)]^H \tilde{\mathbf{x}}(l) - 1 \right\}^2. \quad (26)$$

Assuming the optimal reduced-rank weight vector $\bar{\mathbf{w}}_{\text{gsc}}$ and the transformation matrix $\mathbf{T}_{\text{gsc}}(i)$ are known, respectively, computing the gradients of (26) with respect to $\mathbf{T}_{\text{gsc}}(i)$ and $\bar{\mathbf{w}}_{\text{gsc}}(i)$, and equating them equal to null, we have

$$\mathbf{T}_{\text{gsc}}(i+1) = \hat{\mathbf{R}}_{\tilde{\mathbf{x}}_B}^{-1}(i) \hat{\mathbf{p}}_B(i) \frac{\bar{\mathbf{w}}_{\text{gsc}}^H(i)}{\|\bar{\mathbf{w}}_{\text{gsc}}(i)\|^2}, \quad (27)$$

$$\bar{\mathbf{w}}_{\text{gsc}}(i+1) = \hat{\mathbf{R}}_{\tilde{\mathbf{x}}_B}^{-1}(i) \hat{\mathbf{p}}_B(i), \quad (28)$$

where $\hat{\mathbf{R}}_{\tilde{\mathbf{x}}_B}(i) = \sum_{l=1}^i \alpha^{i-l} \mathbf{B} \tilde{\mathbf{x}}(l) \tilde{\mathbf{x}}^H(l) \mathbf{B}^H$, $\hat{\mathbf{R}}_{\tilde{\mathbf{x}}_B}(i) = \mathbf{T}_{\text{gsc}}^H(i) \hat{\mathbf{R}}_{\tilde{\mathbf{x}}_B}(i) \mathbf{T}_{\text{gsc}}(i)$, $\hat{\mathbf{p}}_B(i) = \sum_{l=1}^i \alpha^{i-l} [d_0^*(l) - 1] \tilde{\mathbf{x}}_B(l)$, and $\hat{\mathbf{p}}_B(i) = \mathbf{T}_{\text{gsc}}^H(i) \hat{\mathbf{p}}_B(i)$.

Setting $\hat{\mathbf{\Phi}}_{\tilde{\mathbf{x}}_B}(i) = \hat{\mathbf{R}}_{\tilde{\mathbf{x}}_B}^{-1}(i)$ and $\hat{\mathbf{\Phi}}_{\tilde{\mathbf{x}}_B}(i) = \hat{\mathbf{R}}_{\tilde{\mathbf{x}}_B}^{-1}(i)$ and employing the matrix inversion lemma yields,

$$\mathbf{T}_{\text{gsc}}(i+1) = \mathbf{T}_{\text{gsc}}(i) - \mathbf{k}_B(i) e_{\bar{\mathbf{w}}_{\text{gsc}}}(i), \quad (29)$$

$$\bar{\mathbf{w}}_{\text{gsc}}(i+1) = \bar{\mathbf{w}}_{\text{gsc}}(i) - e_{\text{gsc}}^*(i) \bar{\mathbf{k}}_B(i), \quad (30)$$

where $\mathbf{k}_B(i) \in \mathbb{C}^{(m-1) \times 1}$ and $\bar{\mathbf{k}}_B(i) \in \mathbb{C}^{r \times 1}$ are gain vectors, $e_{\bar{\mathbf{w}}_{\text{gsc}}}(i) = [1 - \tilde{\mathbf{x}}^H(i) \mathbf{w}(i)] \frac{\bar{\mathbf{w}}_{\text{gsc}}^H(i)}{\|\bar{\mathbf{w}}_{\text{gsc}}(i)\|^2}$, $e_{\text{gsc}}(i) = 1 - \mathbf{w}^H(i) \tilde{\mathbf{x}}(i)$, and $\mathbf{w}(i)$ is defined by (9). A summary of the reduced-rank RLS algorithm with the CCM design for the GSC is given in Table IV.

C. Gram-Schmidt Technique for Problem 2

As mentioned before, the transformation matrix $\mathbf{T}_r(i+1)$ for the DFP is constituted by a bank of full-rank filters $\mathbf{t}_j(i+1)$ ($j = 1, \dots, r$), which cannot be guaranteed to be orthogonal. According to the optimization problem 2 in

TABLE IV
THE JIO-CCM-RLS ALGORITHM FOR GSC

Initialization:
$\mathbf{T}_{\text{gsc}}(1) = [\mathbf{I}_{r \times r} \ \mathbf{0}_{r \times (m-r)}]^T$, $\bar{\mathbf{w}}_{\text{gsc}}(1) = \mathbf{I}_{r \times 1}$
$\hat{\Phi}_{\bar{\mathbf{x}}_B}(0) = \delta \mathbf{I}_{m \times m}$, $\hat{\Phi}_{\bar{\mathbf{x}}_B}(0) = \bar{\delta} \mathbf{I}_{r \times r}$.
Update for each time instant i
$\mathbf{w}(i) = \mathbf{a}_\gamma(\theta_0) - \mathbf{B}^H \mathbf{T}_{\text{gsc}}(i) \bar{\mathbf{w}}_{\text{gsc}}(i)$, $y_{\text{gsc}}(i) = \mathbf{w}^H(i) \mathbf{x}(i)$
$\tilde{\mathbf{x}}(i) = y_{\text{gsc}}^*(i) \mathbf{x}(i)$, $\tilde{\mathbf{x}}_B(i) = \mathbf{B} \tilde{\mathbf{x}}(i)$, $e_{\text{gsc}}(i) = 1 - \mathbf{w}^H(i) \tilde{\mathbf{x}}(i)$
$\mathbf{k}_B(i) = \frac{\alpha^{-1} \hat{\Phi}_{\bar{\mathbf{x}}_B}(i-1) \tilde{\mathbf{x}}_B(i)}{1 + \alpha^{-1} \tilde{\mathbf{x}}_B^H(i) \hat{\Phi}_{\bar{\mathbf{x}}_B}(i-1) \tilde{\mathbf{x}}_B(i)}$
$\hat{\Phi}_{\bar{\mathbf{x}}_B}(i) = \alpha^{-1} \hat{\Phi}_{\bar{\mathbf{x}}_B}(i-1) - \alpha^{-1} \mathbf{k}_B(i) \tilde{\mathbf{x}}_B^H(i) \hat{\Phi}_{\bar{\mathbf{x}}_B}(i-1)$
$e_{\bar{\mathbf{w}}_{\text{gsc}}}(i) = [1 - \tilde{\mathbf{x}}^H(i) \mathbf{w}(i)] \frac{\bar{\mathbf{w}}_{\text{gsc}}^H(i)}{\ \bar{\mathbf{w}}_{\text{gsc}}(i)\ ^2}$
$\mathbf{T}_{\text{gsc}}(i+1) = \mathbf{T}_{\text{gsc}}(i) - \mathbf{k}_B(i) e_{\bar{\mathbf{w}}_{\text{gsc}}}(i)$
$\bar{\mathbf{x}}_B(i) = \mathbf{T}_{\text{gsc}}^H(i+1) \tilde{\mathbf{x}}_B(i)$
$\bar{\mathbf{k}}_B(i) = \frac{\alpha^{-1} \hat{\Phi}_{\bar{\mathbf{x}}_B}(i-1) \bar{\mathbf{x}}_B(i)}{1 + \alpha^{-1} \bar{\mathbf{x}}_B^H(i) \hat{\Phi}_{\bar{\mathbf{x}}_B}(i-1) \bar{\mathbf{x}}_B(i)}$
$\hat{\Phi}_{\bar{\mathbf{x}}_B}(i) = \alpha^{-1} \hat{\Phi}_{\bar{\mathbf{x}}_B}(i-1) - \alpha^{-1} \bar{\mathbf{k}}_B(i) \bar{\mathbf{x}}_B^H(i) \hat{\Phi}_{\bar{\mathbf{x}}_B}(i-1)$
$\mathbf{w}(i) = \mathbf{a}_\gamma(\theta_0) - \mathbf{B}^H \mathbf{T}_{\text{gsc}}(i+1) \bar{\mathbf{w}}_{\text{gsc}}(i)$
$e_{\text{gsc}}(i) = 1 - \mathbf{w}^H(i) \tilde{\mathbf{x}}(i)$
$\bar{\mathbf{w}}_{\text{gsc}}(i+1) = \bar{\mathbf{w}}_{\text{gsc}}(i) - e_{\text{gsc}}^*(i) \bar{\mathbf{k}}_B(i)$

(12), the transformation matrix $\mathbf{T}_r(i)$ can be reformulated to compose r orthogonal vectors, which span the same subspace generated by the original vectors. The reformulation ensures that the projection of the received vector onto each dimension is one time and avoids the overlap (e.g., takes the same information twice or more). Compared with the original transformation matrix, the reformulated transformation matrix is more efficient to keep the useful information in the generated reduced-rank received vector for the parameter estimation. The orthogonal procedure is realized by the Gram-Schmidt (GS) technique [49]. Specifically, after the iterative processes for the computation of the transformation matrix, the GS technique is performed to modify the columns of the transformation matrix as follows:

$$\mathbf{t}_{j,\text{ort}}(i+1) = \mathbf{t}_j(i+1) - \sum_{l=1}^{j-1} \text{proj}_{\mathbf{t}_{l,\text{ort}}(i+1)} \mathbf{t}_j(i+1), \quad (31)$$

where $\mathbf{t}_{j,\text{ort}}(i+1)$ is the normalized orthogonal vector after the GS process. The projection operator is $\text{proj}_{\mathbf{t}_{l,\text{ort}}(i+1)} \mathbf{t}_j(i+1) = [\mathbf{t}_{l,\text{ort}}^H(i+1) \mathbf{t}_{l,\text{ort}}(i+1)]^{-1} [\mathbf{t}_{l,\text{ort}}^H(i+1) \mathbf{t}_j(i+1)] \mathbf{t}_{l,\text{ort}}(i+1)$.

The reformulated transformation matrix $\mathbf{T}_{r,\text{ort}}(i+1)$ is constructed after we obtain a set of orthogonal $\mathbf{t}_{j,\text{ort}}(i+1)$. By employing $\mathbf{T}_{r,\text{ort}}(i+1)$ to compute the reduced-rank weight vectors, the adaptive algorithms could achieve an improved performance. Following the same procedures, we can also apply the GS technique to the adaptive algorithms for the GSC structure. Simulations will be given to show this result. We denominate the GS version of the SG and RLS algorithms as JIO-CCM-GS and JIO-CCM-RGS, respectively.

D. Automatic Rank Selection

The selection of the rank r impacts the performance of the proposed reduced-rank algorithms. Here, we introduce an adaptive method for selecting the rank. Related works on the rank selection for the MSWF and the AVF techniques have been reported in [27] and [50], respectively. Unlike these methods, we describe a rank selection method based on the CM

criterion computed by the filters $\mathbf{T}_r^{(r)}(i)$ and $\bar{\mathbf{w}}^{(r)}(i)$, where the superscript $(\cdot)^{(r)}$ denotes the rank used for the adaptation at each time instant. We consider the rank adaptation technique for both the DFP and the GSC structures. Specifically, in the DFP structure, the rank is automatically selected for the proposed algorithms based on the exponentially-weighted a *posteriori* least-squares cost function according to the CM criterion, which is

$$J_{\text{pcm}}(\mathbf{T}_r^{(r)}(i-1), \bar{\mathbf{w}}^{(r)}(i-1)) = \sum_{l=1}^i \varrho^{i-l} [|\bar{\mathbf{w}}^{(r)H}(l-1) \mathbf{T}_r^{(r)}(l-1) \mathbf{x}(l)|^2 - 1]^2, \quad (32)$$

where ϱ is the exponential weight factor that is required as the optimal rank r can change as a function of the time instant i . From the expressions in Table I and Table III, the key quantities to be updated for the rank adaptation are the transformation matrix $\mathbf{T}_r(i)$, the reduced-rank weight vector $\bar{\mathbf{w}}(i)$, the associated reduced-rank steering vector $\bar{\mathbf{a}}(\theta_0)$ and the matrix $\hat{\Phi}(i)$ (for RLS only). To this end, we express $\mathbf{T}_r^{(r)}(i)$ and $\bar{\mathbf{w}}^{(r)}(i)$ for the rank adaptation as follows:

$$\mathbf{T}_r^{(r)}(i) = \begin{bmatrix} t_{1,1} & t_{1,2} & \dots & t_{1,r_{\min}} & \dots & t_{1,r_{\max}} \\ t_{2,1} & t_{2,2} & \dots & t_{2,r_{\min}} & \dots & t_{2,r_{\max}} \\ \vdots & \vdots & \vdots & \vdots & \vdots & \vdots \\ t_{m,1} & t_{m,2} & \dots & t_{m,r_{\min}} & \dots & t_{m,r_{\max}} \end{bmatrix}, \quad (33)$$

$$\bar{\mathbf{w}}^{(r)}(i) = [\bar{w}_1 \ \bar{w}_2 \ \dots \ \bar{w}_{r_{\min}} \ \dots \ \bar{w}_{r_{\max}}]^T,$$

where r_{\min} and r_{\max} are the minimum and maximum ranks allowed, respectively.

For each time instant i , $\mathbf{T}_r^{(r)}(i)$ and $\bar{\mathbf{w}}^{(r)}(i)$ are updated along with the associated quantities $\bar{\mathbf{a}}(\theta_0)$ and $\hat{\Phi}(i)$ for a selected r according to the minimization of the cost function in (32). The developed automatic rank selection method is given by

$$r_{\text{opt}} = \arg \min_{r_{\min} \leq j \leq r_{\max}} J_{\text{pcm}}(\mathbf{T}_r^{(j)}(i-1), \bar{\mathbf{w}}^{(j)}(i-1)), \quad (34)$$

where j is an integer ranging between r_{\min} and r_{\max} . Note that a smaller rank may provide faster adaptation during the initial stages of the estimation procedure and a slightly larger rank tends to yield a better steady-state performance. Our studies reveal that the range for which the rank r of the proposed algorithms have a positive impact on the performance is very limited, being from $r_{\min} = 3$ to $r_{\max} = 7$. These values are rather insensitive to the number of users in the system, to the number of sensor elements, and work efficiently for the studied scenarios. The additional complexity of this automatic rank selection technique is for the update of involved quantities with the maximum allowed rank r_{\max} and the computation of the cost function in (32). With the case of large m , the rank r is significantly smaller than m and the additional computations do not increase the computational cost significantly.

The proposed algorithms with the rank adaptation technique can increase the convergence rate and improve the output performance, and r can be made fixed once the algorithms reach the steady-state. Simulation results will show how the developed rank adaptation technique works. Note that the same

idea can be employed in the algorithms for the GSC structure. We omit this part for simplification and readability.

V. ANALYSIS OF THE PROPOSED ALGORITHMS

In this section, we provide a complexity analysis of the proposed reduced-rank algorithms and compare them with existing algorithms. An analysis of the optimization problem for the proposed reduced-rank scheme is also carried out.

A. Complexity Analysis

We evaluate the computational complexity of the proposed reduced-rank algorithms and compare them with the existing full-rank and reduced-rank algorithms based on the MSWF and the AVF techniques for the DFP and the GSC structures. With respect to each algorithm, we consider the CMV and the CCM design criteria. The computational requirements are described in terms of the number of complex arithmetic operations, namely, additions and multiplications. The complexity of the proposed and existing algorithms for the DFP is depicted in Table V and for the GSC in Table VI. Since we did not consider the AVF technique for the GSC structure, we put its complexity for the DFP in both tables for comparison.

For the DFP structure, we can say that the complexity of the proposed reduced-rank SG type and extended GS version algorithms increases linearly with rm . The parameter m is more influential since r is selected around a small range that is much less than m for large arrays. The complexity of the proposed reduced-rank RLS type and GS version algorithms is higher than that of the SG type and quadratic with m and r . For the GSC structure, the complexity of the SG type algorithms has extra m^2 terms as compared to the DFP structure in terms of additions and multiplications due to the blocking matrix in the sidelobe canceller. There is no significant difference in complexity of the RLS type algorithms due to the presence of the blocking matrix since (29) and (30) are recursive expressions and, as compared to non-recursive versions, reduce the complexity.

In order to illustrate the main trends in what concerns the complexity of the proposed algorithms, we show in Fig. 3 and Fig. 4 the complexity of both the DFP and the GSC structures in terms of additions and multiplications versus the length of the filter m . Since the complexity of the current algorithms according to the CMV criterion is a little less than that of the CCM criterion, we only plot the curves for the CCM criterion for simplification. Note that the values of r are different with respect to different algorithms, which are set to make the corresponding algorithms reach the best performance according to the experiments. The specific values are given in the figures. It is clear that the proposed SG type and extended GS version algorithms have a complexity slightly higher than the full-rank SG algorithm but much less than the existing algorithms based on the MSWF and the AVF techniques for both the DFP and the GSC structures. The curves of the proposed RLS type and GS version algorithms are situated between the full-rank RLS and the MSWF RLS algorithms in both figures.

TABLE V
COMPUTATIONAL COMPLEXITY OF ALGORITHMS FOR DFP

Algorithm	Additions	Multiplications
FR-CMV-SG	$3m - 1$	$4m + 1$
FR-CCM-SG	$3m$	$4m + 3$
FR-CMV-RLS	$4m^2 - m - 1$	$5m^2 + 5m - 1$
FR-CCM-RLS	$5m^2 + 2m - 1$	$6m^2 + 6m + 3$
MSWF-CMV-SG	$rm^2 + (r + 1)m$ $+ 2r - 2$	$rm^2 + 2rm$ $+ 5r + 2$
MSWF-CCM-SG	$rm^2 + (r + 1)m$ $+ 4r - 2$	$rm^2 + 2rm$ $+ 4r + 4$
MSWF-CMV-RLS	$rm^2 + (r + 1)m$ $+ 4r^2 - 3r - 1$	$(r + 1)m^2 + 2rm$ $+ 5r^2 + 4r$
MSWF-CCM-RLS	$rm^2 + (r + 1)m$ $+ 5r^2 - r$	$(r + 1)m^2 + 2rm$ $+ 6r^2 + 7r + 3$
AVF	$(4r + 5)m^2 + (r - 1)m$ $- 2r - 1$	$(5r + 8)m^2$ $+ (3r + 2)m$
JIO-CMV-SG	$4rm + m + 2r - 3$	$4rm + m + 7r + 3$
JIO-CMV-GS	$7rm - m - 1$	$7rm - 2m + 8r + 2$
JIO-CCM-SG	$4rm + m + 2r - 2$	$4rm + m + 7r + 6$
JIO-CCM-GS	$7rm - m$	$7rm - 2m + 8r + 5$
JIO-CMV-RLS	$4m^2 + (2r - 1)m$ $+ 4r^2 - 4r - 1$	$5m^2 + (3r + 3)m$ $+ 6r^2 + 4r$
JIO-CMV-RGS	$4m^2 + (5r - 3)m$ $+ 4r^2 - 6r + 1$	$5m^2 + 6rm$ $+ 6r^2 + 5r - 1$
JIO-CCM-RLS	$5m^2 + rm$ $+ 5r^2 + 3r - 1$	$6m^2 + (2r + 6)m$ $+ 5r^2 + 9r + 3$
JIO-CCM-RGS	$5m^2 + (4r - 2)m$ $+ 5r^2 + r + 1$	$6m^2 + (5r + 3)m$ $+ 5r^2 + 10r + 2$

TABLE VI
COMPUTATIONAL COMPLEXITY OF ALGORITHMS FOR GSC

Algorithm	Additions	Multiplications
FR-CMV-SG	$m^2 + m - 2$	$m^2 + 2m - 1$
FR-CCM-SG	$m^2 + m - 1$	$m^2 + 2m + 1$
FR-CMV-RLS	$4m^2 - 6m + 4$	$5m^2 - 4m$
FR-CCM-RLS	$4m^2 - 6m + 2$	$5m^2 - 3m$
MSWF-CMV-SG	$(r + 1)m^2 - 2rm$ $+ 2r - 1$	$(r + 2)m^2 - (r + 2)m$ $+ 2r + 2$
MSWF-CCM-SG	$(r + 1)m^2 - 2rm + 2r$	$(r + 2)m^2 - (r + 2)m$ $+ 2r + 4$
MSWF-CMV-RLS	$(r + 1)m^2 - 2rm$ $+ 3r^2 + r - 1$	$(r + 2)m^2 - (r + 2)m$ $+ 4r^2 + 4r$
MSWF-CCM-RLS	$(r + 1)m^2 - 2rm$ $+ 3r^2 + r - 1$	$(r + 2)m^2 - (r + 1)m$ $+ 4r^2 + 4r + 1$
AVF	$(4r + 5)m^2 + (r - 1)m$ $- 2r - 1$	$(5r + 8)m^2$ $+ (3r + 2)m$
JIO-CMV-SG	$m^2 + 2rm - m - r$	$m^2 + 2rm + r + 2$
JIO-CMV-GS	$m^2 + 5rm - 3m$ $- 6r + 4$	$m^2 + 5rm - 3m$ $- r + 4$
JIO-CCM-SG	$m^2 + 2rm - m - r + 1$	$m^2 + 2rm + r + 4$
JIO-CCM-GS	$m^2 + 5rm - 3m$ $- 6r + 5$	$m^2 + 5rm - 3m$ $- r + 6$
JIO-CMV-RLS	$4m^2 + (2r - 8)m$ $+ 5r^2 - 2r + 4$	$5m^2 + (2r - 6)m$ $+ 7r^2 + 3r + 2$
JIO-CMV-RGS	$4m^2 + (5r - 10)m$ $+ 5r^2 - 7r + 8$	$5m^2 + (5r - 9)m$ $+ 7r^2 + r + 4$
JIO-CCM-RLS	$4m^2 + (2r - 7)m$ $+ 5r^2 - 4r + 3$	$5m^2 + (2r - 4)m$ $+ 7r^2 + 2r + 1$
JIO-CCM-RGS	$4m^2 + (5r - 9)m$ $+ 5r^2 - 9r + 7$	$5m^2 + (5r - 7)m$ $+ 7r^2 + 3$

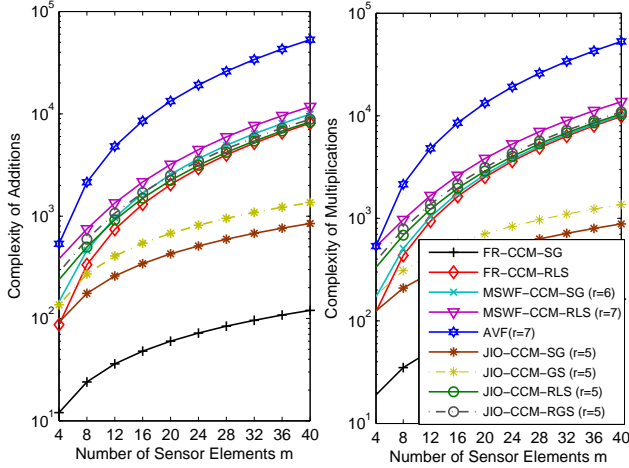


Fig. 3. Complexity in terms of arithmetic operations versus the length of the filter m for the DFP structure.

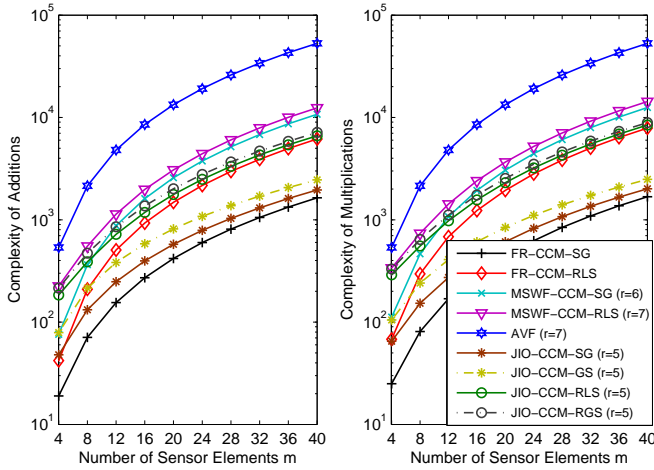


Fig. 4. Complexity in terms of arithmetic operations versus the length of the filter m for the GSC structure.

B. Analysis of the Optimization Problem

Here, we present the analysis of the proposed reduced-rank scheme according to the CCM criterion, which depends on the transformation matrix and the reduced-rank weight vector. Our approach starts from the analysis of the full-rank constant modulus criterion and then utilizes the transformation matrix and the reduced-rank weight vector with the received vector to express the output. The constraint is enforced during the analysis. We will consider the analysis for both the DFP and the GSC structures.

The full-rank constant modulus cost function in (2) with $p = 2$ and $\nu = 1$ can be written as

$$\begin{aligned} J_{\text{cm}}(\mathbf{w}(i)) &= \mathbb{E}[|y(i)|^4 - 2|y(i)|^2 + 1] \\ &= \mathbb{E}[|\mathbf{w}^H(i)\mathbf{x}(i)\mathbf{x}^H(i)\mathbf{w}(i)|^2] \\ &\quad - 2\mathbb{E}[|\mathbf{w}^H(i)\mathbf{x}(i)|^2] + 1, \end{aligned} \quad (35)$$

where $\mathbf{x}(i) = \sum_{k=0}^{q-1} C_k d_k(i) \mathbf{a}(\theta_k) + \mathbf{n}(i)$ ($k = 0, \dots, q-1$)

from (1) with D_k being the signal amplitude and d_k is the transmitted bit of the k th user. Note that we have replaced s_k in (1) by $C_k d_k$.

For the sake of analysis, we will follow the assumption in [51] and consider a noise free case. For small noise variance σ_n^2 , this assumption can be considered as a small perturbation and the analysis will still be applicable. For large σ_n^2 , we remark that the term γ can be adjusted for the analysis. Under this assumption, we write the received vector as $\mathbf{x}(i) = \mathbf{A}(\boldsymbol{\theta})\mathbf{C}\mathbf{d}(i)$, where $\mathbf{A}(\boldsymbol{\theta})$, as before, denotes the signature matrix, $\mathbf{C}(i) = \text{diag}[C_0, \dots, C_{q-1}] \in \mathbb{C}^{q \times q}$, and $\mathbf{d}(i) = [d_0(i), \dots, d_{q-1}(i)]^T \in \mathbb{C}^{q \times 1}$.

For simplicity, we drop the time instant in the quantities. Letting $\varsigma_k = C_k \mathbf{w}^H \mathbf{a}(\theta_k)$ and $\boldsymbol{\varsigma} = [\varsigma_0, \dots, \varsigma_{q-1}]^T$, we have

$$J_{\text{cm}} = \mathbb{E}[\boldsymbol{\varsigma}^H \mathbf{d} \mathbf{d}^H \boldsymbol{\varsigma} \boldsymbol{\varsigma}^H \mathbf{d} \mathbf{d}^H \boldsymbol{\varsigma}] - 2\mathbb{E}[\boldsymbol{\varsigma}^H \mathbf{d} \mathbf{d}^H \boldsymbol{\varsigma}] + 1. \quad (36)$$

Since d_k are independent random variables, the evaluation of the first two terms in the brackets in (36) reads

$$\begin{aligned} \boldsymbol{\varsigma}^H \mathbf{d} \mathbf{d}^H \boldsymbol{\varsigma} \boldsymbol{\varsigma}^H \mathbf{d} \mathbf{d}^H \boldsymbol{\varsigma} &= \sum_{k=0}^{q-1} \sum_{l=0}^{q-1} |d_k|^2 |d_l|^2 \varsigma_k^* \varsigma_k \varsigma_l^* \varsigma_l, \\ \boldsymbol{\varsigma}^H \mathbf{d} \mathbf{d}^H \boldsymbol{\varsigma} &= \sum_{k=0}^{q-1} |d_k|^2 \varsigma_k^* \varsigma_k. \end{aligned} \quad (37)$$

For the reduced-rank scheme with the DFP structure, we have $\mathbf{w} = \mathbf{T}_r \bar{\mathbf{w}}$. Thus,

$$\varsigma_k = C_k (\mathbf{T}_r \bar{\mathbf{w}})^H \mathbf{a}(\theta_k) = C_k \sum_{j=1}^r \mathbf{t}_{\bar{w}_j}^H \mathbf{a}(\theta_k), \quad (38)$$

where $\mathbf{t}_{\bar{w}_j} = \bar{w}_j \mathbf{t}_j \in \mathbb{C}^{m \times 1}$ and \mathbf{t}_j ($j = 1, \dots, r$) is the column vector of the transformation matrix \mathbf{T}_r .

Given $t_j(\theta_k) = C_k \mathbf{t}_{\bar{w}_j}^H \mathbf{a}(\theta_k)$ and $\varsigma_k = \sum_{j=1}^r t_j(\theta_k)$, we get

$$\varsigma_k^* \varsigma_k = \sum_{j=1}^r \sum_{n=1}^r t_j^*(\theta_k) t_n(\theta_k). \quad (39)$$

From (38) and the constraint condition in (11), it is interesting to find $\varsigma_0 = C_0 \gamma$. Substituting this expression and (38) into (37), we have

$$\begin{aligned} \boldsymbol{\varsigma}^H \mathbf{d} \mathbf{d}^H \boldsymbol{\varsigma} &= |d_0|^2 \varsigma_0^* \varsigma_0 + \sum_{k=1}^{q-1} |d_k|^2 \varsigma_k^* \varsigma_k \\ &= |d_0|^2 C_0^2 \gamma^2 + \tilde{\boldsymbol{\zeta}}^H \tilde{\mathbf{d}} \tilde{\boldsymbol{\zeta}}, \end{aligned} \quad (40)$$

where $\tilde{\boldsymbol{\zeta}} = [\varsigma_1, \dots, \varsigma_{q-1}]^T \in \mathbb{C}^{(q-1) \times 1}$ and $\tilde{\mathbf{d}} = [d_1, \dots, d_{q-1}]^T \in \mathbb{C}^{(q-1) \times 1}$.

Substituting (40) into (36), we get the CCM cost function in the form of reduced-rank, i.e.,

$$\begin{aligned} J_{\text{ccm}} &= \mathbb{E}[|d_0|^2 C_0^2 \gamma^2 + \tilde{\boldsymbol{\zeta}}^H \tilde{\mathbf{d}} \tilde{\boldsymbol{\zeta}}]^2 \\ &\quad - 2\mathbb{E}[|d_0|^2 C_0 \gamma^2 + \tilde{\boldsymbol{\zeta}}^H \tilde{\mathbf{d}} \tilde{\boldsymbol{\zeta}}] + 1, \end{aligned} \quad (41)$$

where $\tilde{\boldsymbol{\zeta}}$ is a function of the transformation matrix and the reduced-rank weight vector, as shown in (38). This expression is important for the reduced-rank CCM analysis. The fact that \mathbf{T}_r and $\bar{\mathbf{w}}$ depend on each other and exchange information claims that we need to take both of them into consideration for the analysis. The expression in (38) combines these two

quantities together and thus circumvents the complicated procedures of performing the analysis separately. Note that (41) is a constrained expression since the constraint condition has been enclosed in the first term of each bracket.

We can examine the convexity of (11) by computing the Hessian matrix \mathbf{H} with respect to $\tilde{\zeta}^H$ and $\tilde{\zeta}$, that is $\mathbf{H} = \frac{\partial}{\partial \tilde{\zeta}^H} \frac{\partial J_{\text{ccm}}}{\partial \tilde{\zeta}}$ yields,

$$\mathbf{H} = 2\mathbb{E}[(|d_0|^2 C_0^2 \gamma^2 - 1) \tilde{\mathbf{d}} \tilde{\mathbf{d}}^H + \tilde{\zeta}^H \tilde{\mathbf{d}} \tilde{\mathbf{d}}^H \tilde{\zeta} + \tilde{\zeta} \tilde{\mathbf{d}} \tilde{\mathbf{d}}^H \tilde{\zeta}^H], \quad (42)$$

where \mathbf{H} should be positive semi-definite to ensure the convexity of the optimization problem. The second and third terms in (42) yield positive semi-definite matrices, while the first term provides the condition $|d_0|^2 C_0^2 \gamma^2 - 1 \geq 0$ to ensure the convexity. Thus, J_{ccm} is a convex function of \mathbf{T}_r and $\bar{\mathbf{w}}$ when

$$\gamma^2 \geq \frac{1}{|d_0|^2 C_0^2}. \quad (43)$$

For the reduced-rank scheme with the GSC structure, the expression of the weight vector has been given in (9). Substituting this expression into the definition of ς_k and considering the fact that $\mathbf{B}\mathbf{a}(\theta_0) = \mathbf{0}$, we obtain

$$\varsigma_k = \begin{cases} C_0 \mathbf{a}_\gamma^H(\theta_0) \mathbf{a}(\theta_0) & \text{for } k = 0 \\ -C_k \sum_{j=1}^r \mathbf{t}_{\bar{\mathbf{w}}_{\text{gsc},j}}^H \mathbf{B}\mathbf{a}(\theta_k) & \text{for } k = 1, \dots, q-1 \end{cases}, \quad (44)$$

where $\mathbf{t}_{\bar{\mathbf{w}}_{\text{gsc},j}} = \bar{\mathbf{w}}_{\text{gsc},j} \mathbf{t}_{\text{gsc},j} \in \mathbb{C}^{(m-1) \times 1}$ and $\mathbf{t}_{\text{gsc},j}$ ($j = 1, \dots, r$) is the column vector of \mathbf{T}_{gsc} for the GSC structure.

Given $\mathbf{t}'_{j,l}(\theta_k) = C_k a_l(\theta_k) \mathbf{t}_{\bar{\mathbf{w}}_{\text{gsc},j}}^H \mathbf{b}_l$ ($l = 1, \dots, m$), where $a_n(\theta_k)$ is the l th element of the steering vector with the direction θ_k and $\mathbf{b}_l \in \mathbb{C}^{(m-1) \times 1}$ is the l th column vector of the signal blocking matrix \mathbf{B} , we have $\varsigma_k = -\sum_{n=1}^m \sum_{j=1}^r \mathbf{t}'_{j,n}(\theta_k)$. Thus, for $k = 1, \dots, q-1$,

$$\varsigma_k^* \varsigma_k = \sum_{j=1}^r \sum_{n=1}^m \sum_{l=1}^m \sum_{p=1}^m \mathbf{t}'_{j,l}(\theta_k)^* \mathbf{t}'_{n,p}(\theta_k). \quad (45)$$

Substituting (44) and (45) into (37), we get the expression for the GSC structure, which is

$$\begin{aligned} \boldsymbol{\varsigma}^H \mathbf{d} \mathbf{d}^H \boldsymbol{\varsigma} &= |d_0|^2 \varsigma_0^* \varsigma_0 + \sum_{k=1}^{q-1} |d_k|^2 \varsigma_k^* \varsigma_k \\ &= |d_0|^2 C_0^2 \mathbf{a}^H(\theta_0) \mathbf{a}_\gamma(\theta_0) \mathbf{a}^H(\theta_0) \mathbf{a}(\theta_0) + \tilde{\zeta}^H \tilde{\mathbf{d}} \tilde{\mathbf{d}}^H \tilde{\zeta} \\ &= |d_0|^2 C_0^2 \gamma^2 + \tilde{\zeta}^H \tilde{\mathbf{d}} \tilde{\mathbf{d}}^H \tilde{\zeta}, \end{aligned} \quad (46)$$

which is in the same form as in (40) for the DFP structure but with the different expression of the quantity $\tilde{\zeta}$. Using the similar interpretation for the DFP, the quantity ς_k in (44) combines the transformation matrix and the reduced-rank weight vector together and thus simplifies the analysis. By computing the Hessian matrix \mathbf{H} , we can obtain the same conclusion as shown in (43).

VI. SIMULATIONS

In this section, we evaluate the output signal-to-interference-plus-noise ratio (SINR) performance of the proposed adaptive reduced-rank algorithms and compare them with the existing

methods. Specifically, we compare the proposed SG and RLS type algorithms with the full-rank (FR) SG and RLS and reduced-rank methods based on the MSWF and the AVF techniques for both the DFP and the GSC structures. With respect to each algorithm, we consider the CMV and the CCM criteria for the beamformer design. We assume that the DOA of the desired user is known by the receiver. In each experiment, a total of $K = 1000$ runs are carried out to get the curves. For all simulations, the source power (including the desired user and interferers) is $\sigma_s^2 = \sigma_i^2 = 1$, the input signal-to-noise (SNR) ratio is SNR=10 dB with spatially and temporally white Gaussian noise, and $\gamma = 1$. Simulations are performed by an ULA containing $m = 32$ sensor elements with half-wavelength interelement spacing.

A. Comparison of CMV and CCM Based Algorithms

In this part, we compare the proposed and existing algorithms according to the CMV and the CCM criteria for the DFP structure of the beamformer design. The simulation, which includes two experiments, shows the input SNR versus the output SINR. The input SNR is varied between -10 dB and 10 dB. The number of users is $q = 5$ with one desired user. Fig. 5 (a) plots the curves of the SG type algorithms based on the full-rank, MSWF, AVF and the proposed reduced-rank scheme, and Fig. 5 (b) shows the corresponding RLS type algorithms. The parameters used to obtain these curves are given and the rank r is selected to optimize the algorithms. From Fig. 5 (a), the output SINR of all SG type methods increases following the increase of the input SNR. The algorithms based on the CCM beamformer design outperform those based on the CMV since the CCM criterion is a positive measure of the beamformer output deviating from a constant modulus, which provides more information than the CMV for the parameter estimation of constant modulus constellations. The proposed CCM algorithms achieve better performance than the existing full-rank, MSWF and AVF ones. By employing the GS technique to reformulate the transformation matrix, the GS version algorithms achieve improved performance. Fig. 5 (b) verifies the same fact but for the RLS type algorithms. It is clear that the RLS type algorithms superior to the SG type ones for all input SNR values.

This simulation verifies that the performance of the adaptive algorithms based on the CCM beamformer design has a similar trend but is better than that based on the CMV for constant modulus constellations. Considering this fact, we will only compare the CCM based adaptive algorithms in the following part for simplification. Note that all the methods in this simulation are for the DFP structure. The algorithms for the GSC structure show a similar performance, which is given in the next part.

B. Output SINR for the DFP and the GSC

We evaluate the output SINR performance of the proposed and existing algorithms against the number of snapshots for both the DFP and the GSC structures in Fig. 6 and Fig. 7, respectively. The number of snapshots is $N = 500$. In Fig. 6, the convergence of the proposed SG type and extended

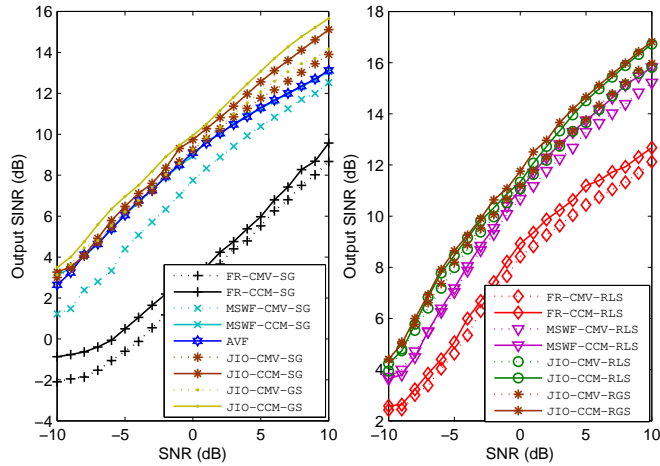


Fig. 5. Output SINR versus input SNR with $m = 32$, $q = 5$, SNR= 10 dB, (a) $\mu_{T_r} = 0.002$, $\mu_{\bar{w}} = 0.001$, $r = 5$ for SG, $\mu_{T_r} = 0.003$, $\mu_{\bar{w}} = 0.0007$, $r = 5$ for GS; (b) $\alpha = 0.998$, $\delta = \bar{\delta} = 0.03$, $r = 5$ for RLS, $\alpha = 0.998$, $\delta = \bar{\delta} = 0.028$, $r = 5$ for RGS of the proposed CCM reduced-rank scheme.

GS version algorithms is close to the RLS type algorithm based on the MSWF, and the output SINR values are higher than other SG type methods based on the full-rank, MSWF and AVF. The convergence of the proposed RLS type and GS version algorithms is slightly slower than the AVF, but much faster than other existing and proposed methods. Its tracking performance outperforms the MSWF and AVF based algorithms.

Fig. 7 is carried out for the GSC structure under the same scenario as in Fig. 6. The curves of the considered algorithms for the GSC show nearly the same convergence and tracking performance as those for the DFP. It implies that the GSC structure is an alternative way for the CCM beamformer design. The difference is that the GSC processor incorporates the constraint in the structure and thus converts the constrained optimization problem into an unconstrained one. The adaptive implementation of the GSC beamformer design is different from that of the DFP but the performance is similar. The following simulations are carried out for the DFP structure to simplify the presentation.

C. Mean Square Estimation Error of the Weight Solution

In Fig. 8, we measure the mean square estimation error $\mathbb{E}\{\|\mathbf{w}(i) - \mathbf{w}_{\text{mvdr}}\|^2\}$ between the weight solutions (full-rank) of the proposed methods $\mathbf{w}(i) = \mathbf{T}_r(i)\bar{\mathbf{w}}(i)$ and that of the minimum-variance-distortionless-response (MVDR) method [3] $\mathbf{w}_{\text{mvdr}} = \gamma \frac{\mathbf{R}^{-1}\alpha(\theta_0)}{\alpha^H(\theta_0)\mathbf{R}^{-1}\alpha(\theta_0)}$, where \mathbf{R} is obtained by its sample-average estimation. The experiment is carried out with the same scenario as in Fig 6. It exhibits that the mean square estimation error decreases following the snapshots. The values of the proposed SG and RLS type algorithms decrease rapidly and reach a relative lower level compared with those of the existing methods. Note that \mathbf{w}_{mvdr} is not an optimum solution for the proposed algorithms but viewed as a referenced weight solution since, for the CCM based algorithm, the weight

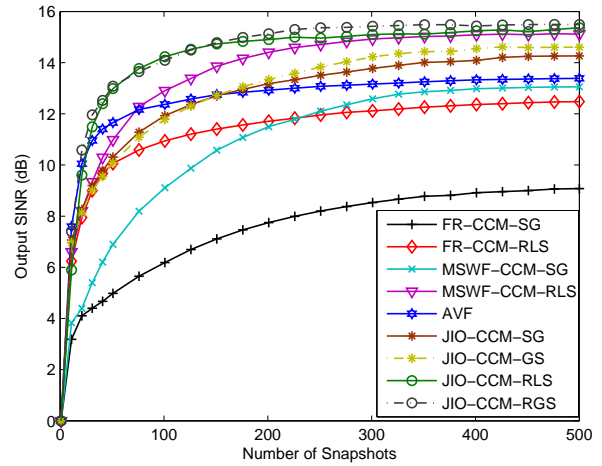


Fig. 6. Output SINR versus the number of snapshots with $m = 32$, $q = 7$, SNR= 10 dB, $\mu_{T_r} = 0.003$, $\mu_{\bar{w}} = 0.003$, $r = 5$ for SG, $\mu_{T_r} = 0.0023$, $\mu_{\bar{w}} = 0.003$, $r = 5$ for GS, $\alpha = 0.998$, $\delta = \bar{\delta} = 0.025$, $r = 5$ for RLS, $\alpha = 0.998$, $\delta = \bar{\delta} = 0.02$, $r = 5$ for RGS of the DFP structure.

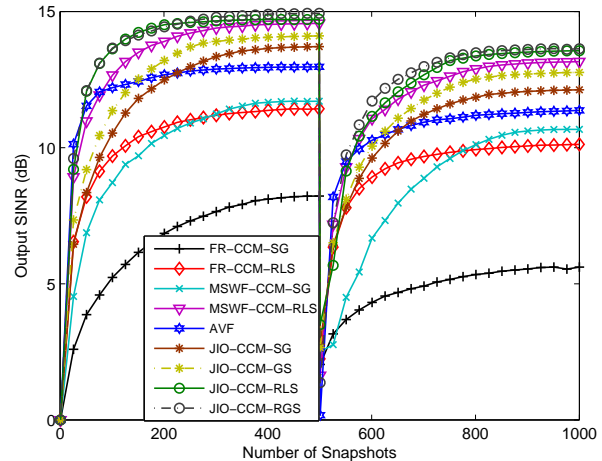


Fig. 7. Output SINR versus input SNR with $m = 32$, $q = 7$, SNR= 10 dB, $\mu_{T_r} = 0.0025$, $\mu_{\bar{w}_{\text{gsc}}} = 0.002$, $r = 5$ for SG, $\mu_{T_r} = 0.003$, $\mu_{\bar{w}_{\text{gsc}}} = 0.003$, $r = 5$ for GS, $\alpha = 0.998$, $\delta = \bar{\delta} = 0.01$, $r = 5$ for RLS, $\alpha = 0.998$, $\delta = \bar{\delta} = 0.0093$, $r = 5$ for RGS of the GSC structure.

expression is not a pure function of the received data but also depends on the previous weighting values.

D. Output SINR versus Rank r and Automatic Rank Selection

In the next two experiments, we assess the output SINR performance of the proposed and analyzed algorithms versus their associated rank r , and check the effectiveness of the automatic rank selection technique. The experiment in Fig. 9 is intended for setting the adequate rank r of the reduced-rank schemes for a given input SNR and number of snapshots. The scenario is the same as that in Fig. 6 except that the number of snapshots is fixed to be $N = 500$ and the rank r is varied between 1 and 16. The result indicates that the best performance of the proposed SG and RLS type algorithms

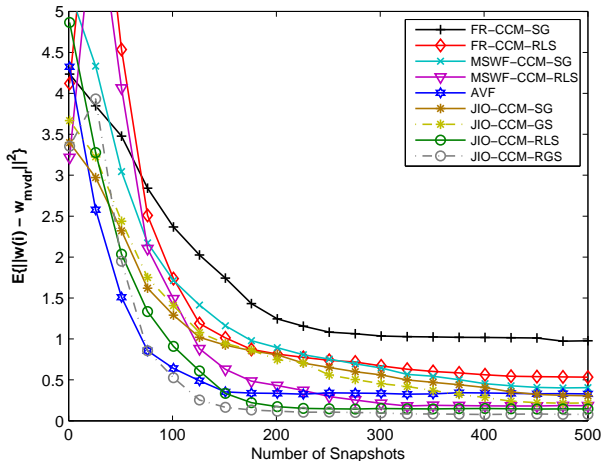


Fig. 8. Square estimation error between the weight solution and the MVDR weight solution.

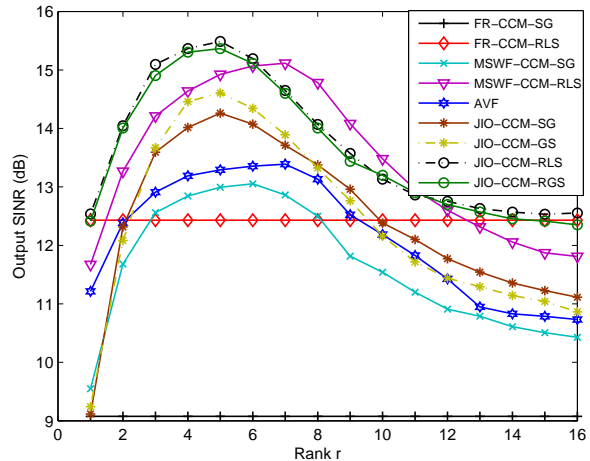


Fig. 9. Output SINR versus rank r with $m = 32$, $q = 7$, $\text{SNR} = 10$ dB.

is obtained with rank $r = 5$ for the proposed reduced-rank scheme. The performance of the full-rank methods is invariant with the change of the rank r . For the MSWF technique, its SG and RLS type algorithms achieve their best performance with ranks $r = 6$ and $r = 7$, respectively. For the AVF-based algorithm, the best rank is found to be $r = 7$. It is interesting to note that the best r is usually much smaller than the number of elements m , which leads to significant computational savings. For the proposed and analyzed algorithms, the range of r that has the best performance is concentrated between $r_{\min} = 3$ and $r_{\max} = 7$. This range is used in the next experiment to check the performance of the proposed algorithms with the automatic rank selection technique.

Since the performance of the proposed reduced-rank algorithms was found in our studies to be a function of the rank r and other parameters such as the step size and the forgetting factor, we need to consider their impacts on the performance of the system. Specifically, we assume that the step size of the SG type algorithms and the forgetting vector of the RLS type algorithms are adequately chosen and we focus on the developed automatic rank selection technique introduced in the previous section.

In Fig. 10, the proposed reduced-rank algorithms utilize fixed values for their rank and also the automatic rank selection technique. We consider the presence of $q = 10$ users (one desired) in the system. The results show that with a lower rank $r = 3$ the reduced-rank algorithms usually converge faster but achieve lower output SINR values. Conversely, with a higher rank $r = 7$ the proposed algorithms converge relatively slower than with a lower rank but reach higher output SINR values. The developed automatic rank selection technique allows the proposed algorithms to circumvent the tradeoff between convergence and steady-state performance for a given rank, by adaptively choosing the best rank for a given number of snapshots which provides both fast convergence and improved tracking performance.

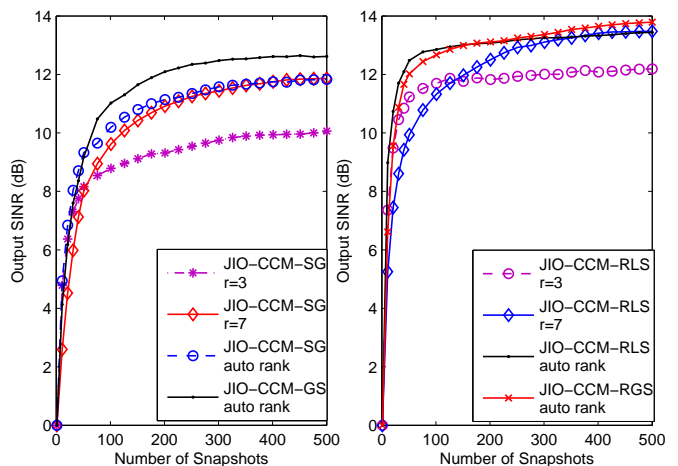


Fig. 10. Output SINR versus the number of snapshots with $m = 32$, $q = 10$, $\text{SNR} = 10$ dB, (a) $\mu_{T_r} = 0.003$, $\mu_{\bar{w}} = 0.004$ for SG, $\mu_{T_r} = 0.003$, $\mu_{\bar{w}} = 0.001$ for GS; (b) $\alpha = 0.998$, $\delta = \bar{\delta} = 0.03$ for RLS, $\alpha = 0.998$, $\delta = \bar{\delta} = 0.026$, $r = 5$ for RGS with the automatic rank selection technique.

E. Performance in non-stationary scenarios

In the last experiment, we evaluate the performance of the proposed and analyzed algorithms in a non-stationary scenario, namely, when the number of users changes. The automatic rank selection technique is employed, and the step size and the forgetting factor are set to ensure that the considered algorithms converge quickly to the steady-state. In this experiment, the scenario starts with $q = 8$ users including one desired user. From the first stage (first 500 snapshots) of Fig. 11, the convergence and steady-state performance of the proposed SG type algorithms is superior to other SG type methods with the full-rank, MSWF and AVF. The proposed RLS type algorithm has a convergence rate a little slower than the AVF but faster than the other analyzed methods, and the steady-state performance better than the existing ones. Three more interferers enter the system at time instant $i = 500$. This

change makes the output SINR reduce suddenly and degrades the performance of all methods. The proposed SG and RLS type algorithms keep faster convergence and better steady-state performance in comparison with the corresponding SG and RLS type methods based on the full-rank and MSWF techniques. The convergence of the AVF method is fast but the steady-state performance is inferior to the proposed methods.

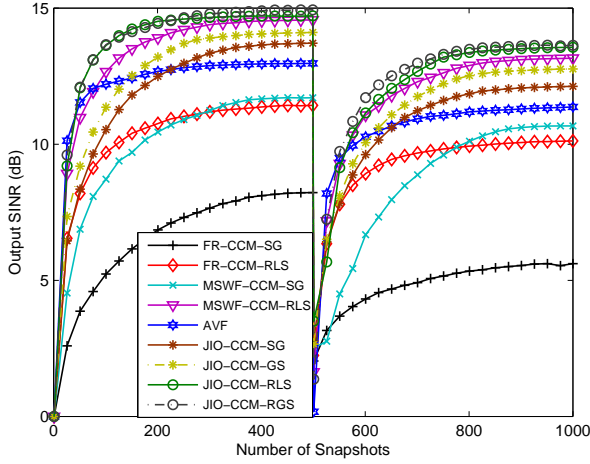


Fig. 11. Output SINR versus input SNR with $m = 32$, $q_1 = 8$, $q_2 = 11$, $\text{SNR} = 10$ dB, $\mu_{T_r} = 0.003$, $\mu_{\bar{w}} = 0.0038$, $r = 5$ for SG, $\mu_{T_r} = 0.003$, $\mu_{\bar{w}} = 0.001$, $r = 5$ for GS, $\alpha = 0.998$, $\delta = \bar{\delta} = 0.033$, $r = 5$ for RLS, $\alpha = 0.998$, $\delta = \bar{\delta} = 0.028$, $r = 5$ for RGS of the proposed CCM reduced-rank scheme.

VII. CONCLUDING REMARKS

We proposed a CCM reduced-rank scheme based on the joint iterative optimization of adaptive filters for beamformer design. In the proposed scheme, the dimension of the received vector is reduced by the adaptive transformation matrix that is formed by a bank of full-rank adaptive filters, and the transformed received vector is processed by the reduced-rank adaptive filter for estimating the desired signal. The proposed scheme was developed for both DFP and GSC structures. We derived the CCM expressions for the transformation matrix and the reduced-rank weight vector, and developed SG and RLS type algorithms for their efficient implementation. The GS technique was employed in the proposed algorithms to reformulate the transformation matrix and thus improve the performance. The automatic rank selection technique was developed to determine the most adequate rank and make a good trade-off between the convergence rate and the steady-state performance for the proposed methods. The complexity and convexity analysis of the proposed algorithms was carried out. Simulation results for the beamforming application showed that the proposed reduced-rank algorithms significantly outperform the existing full-rank and reduced-rank methods in convergence and steady-state performance at comparable complexity.

APPENDIX

DERIVATION OF (24)

In this appendix, we show the details of the derivation of the expression for the transformation matrix in (33). Assuming $\bar{w}(i) \neq \mathbf{0}$ is known, taking the gradient terms of (32) with respect to $T_r(i)$, we get

$$\begin{aligned} \nabla L_{\text{un}T_r(i)} &= 2 \sum_{l=1}^i |y(l)|^2 \mathbf{x}(l) \mathbf{x}^H(l) T_r(i) \bar{w}(i) \bar{w}^H(i) \\ &\quad - 2 \sum_{l=1}^i \mathbf{x}(l) \mathbf{x}^H(l) T_r(i) \bar{w}(i) \bar{w}^H(i) + 2\lambda \mathbf{a}(\theta_0) \bar{w}^H(i) \\ &= 2\hat{\mathbf{R}}(i) T_r(i) \bar{w}(i) \bar{w}^H(i) - 2\hat{\mathbf{p}}(i) \bar{w}^H(i) \\ &\quad + 2\lambda \mathbf{a}(\theta_0) \bar{w}^H(i). \end{aligned} \quad (47)$$

Making the above gradient terms equal to the zero matrix, right-multiplying the both sides by $\bar{w}(i)$, and rearranging the expression, it becomes

$$T_r(i) \bar{w}(i) = \hat{\mathbf{R}}^{-1}(i) [\hat{\mathbf{p}}(i) - \lambda \mathbf{a}(\theta_0)] \quad (48)$$

If we define $\hat{\mathbf{p}}_{\hat{\mathbf{R}}}(i) = \hat{\mathbf{R}}^{-1}(i) [\hat{\mathbf{p}}(i) - \lambda \mathbf{a}(\theta_0)]$, the solution of $T_r(i)$ in (48) can be regarded to find the solution to the linear equation

$$T_r(i) \bar{w}(i) = \hat{\mathbf{p}}_{\hat{\mathbf{R}}}(i) \quad (49)$$

Given a $\bar{w}(i) \neq \mathbf{0}$, there exists multiple $T_r(i)$ satisfying (49) in general. Therefore, we derive the minimum Frobenius-norm solution for stability. Let us express the quantities involved in (49) by

$$T_r(i) = \begin{bmatrix} \bar{\rho}_1(i) \\ \bar{\rho}_2(i) \\ \vdots \\ \bar{\rho}_m(i) \end{bmatrix}; \quad \hat{\mathbf{p}}_{\hat{\mathbf{R}}}(i) = \begin{bmatrix} \hat{p}_{\hat{\mathbf{R}},1}(i) \\ \hat{p}_{\hat{\mathbf{R}},2}(i) \\ \vdots \\ \hat{p}_{\hat{\mathbf{R}},m}(i) \end{bmatrix} \quad (50)$$

The search for the minimum Frobenius-norm solution of (49) is reduced to the following m subproblems ($j = 1, \dots, m$):

$$\min \|\bar{\rho}_j(i)\|^2 \quad \text{subject to} \quad \bar{\rho}_j(i) \bar{w}(i) = \hat{p}_{\hat{\mathbf{R}},j}(i), \quad (51)$$

The solution to (51) is the projection of $\bar{\rho}(i)$ onto the hyperplane $\mathcal{H}_j(i) = \{\bar{\rho}(i) \in \mathbb{C}^{1 \times r} : \bar{\rho}(i) \bar{w}(i) = \hat{p}_{\hat{\mathbf{R}},j}(i)\}$, which is given by

$$\bar{\rho}_j(i) = \hat{p}_{\hat{\mathbf{R}},j}(i) \frac{\bar{w}^H(i)}{\|\bar{w}(i)\|^2} \quad (52)$$

Hence, the minimum Frobenius-norm solution of the transformation matrix is given by

$$T_r(i) = \hat{\mathbf{p}}_{\hat{\mathbf{R}}}(i) \frac{\bar{w}^H(i)}{\|\bar{w}(i)\|^2} \quad (53)$$

Substituting the definition of $\hat{\mathbf{p}}_{\hat{\mathbf{R}}}(i)$ into (53), we have

$$T_r(i) = \hat{\mathbf{R}}^{-1}(i) [\hat{\mathbf{p}}(i) - \lambda \mathbf{a}(\theta_0)] \frac{\bar{w}^H(i)}{\|\bar{w}(i)\|^2} \quad (54)$$

The multiplier λ can be obtained by incorporating (48) with the constraint $\bar{\mathbf{w}}^H(i)\mathbf{T}_r^H(i)\mathbf{a}(\theta_0) = \gamma$, which is

$$\lambda = \frac{\hat{\mathbf{p}}(i)\hat{\mathbf{R}}^{-1}(i)\mathbf{a}(\theta_0) - \gamma}{\mathbf{a}^H(\theta_0)\hat{\mathbf{R}}^{-1}(i)\mathbf{a}(\theta_0)} \quad (55)$$

Therefore, the expression of the transformation matrix in (33) can be obtained by substituting (55) into (54).

REFERENCES

- [1] S. Anderson, M. Millnert, M. Viberg, and B. Wahlberg, "An adaptive array for mobile communication systems," *IEEE Trans. Vehicular Technology*, vol. 40, pp. 230-236, Feb. 1991.
- [2] A. B. Gershman, E. Nemeth, and J. F. Bohme, "Experimental performance of adaptive beamforming in sonar environment with a towed array and moving interfering sources," *IEEE Trans. Signal Processing*, vol. 48, pp. 246-250, Jan. 2000.
- [3] H. L. Van Trees, *Detection, Estimation, and Modulation, Part IV, Optimum Array Processing*, John Wiley & Sons, 2002.
- [4] J. Li and P. Stoica, *Robust Adaptive Beamforming*, Hoboken, NJ: Wiley, 2006.
- [5] S. A. Vorobyov, H. Chen, and A. B. Gershman, "On the Relationship Between Robust Minimum Variance Beamformers With Probabilistic and Worst-Case Distortionless Response Constraints", *IEEE Trans. Signal Processing*, vol. 56, pp. 5719-5724, Nov. 2008.
- [6] O. L. Frost, "An algorithm for linearly constrained adaptive array processing," *IEEE Proc.*, AP-30, pp. 27-34, 1972.
- [7] L. Griffiths and C. Jim, "An alternative approach to linearly constrained adaptive beamforming," *IEEE Trans. Antennas and Propagation*, vol. 30, pp. 27-34, Jan. 1982.
- [8] B. D. Van Veen, "Adaptive convergence of linearly constrained beamformers based on the sample covariance matrix," *IEEE Trans. Signal Processing*, vol. 39, pp. 1470-1473, June 1991.
- [9] L. S. Resende, J. M. T. Romano, and M. G. Bellanger, "A fast least-squares algorithm for linearly constrained adaptive filtering," *IEEE Trans. Signal Processing*, vol. 44, pp. 1168-1174, May 1996.
- [10] Y. Zou, Z. L. Yu, and Z. Lin, "A robust algorithm for linearly constrained adaptive beamforming," *IEEE Signal Processing Letters*, vol. 11, pp. 26-29, Jan. 2004.
- [11] A. Pezeshki, L. L. Scharf, M. R. Azimi-Sadjadi, and Y. Hua, "Two-channel constrained least squares problems: Solutions using power methods and connections with canonical coordinates," *IEEE Trans. Signal Processing*, vol. 53, pp. 121-135, Jan. 2005.
- [12] A. Pezeshki, M. R. Azimi-Sadjadi, and L. L. Scharf, "A network for recursive extraction of canonical coordinates," *Neural Networks*, vol. 16(5-6), pp. 801-808, July 2003.
- [13] J. Via, I. Santamaria, and J. Perez, "A robust RLS algorithm for adaptive canonical correlation analysis," *IEEE Int. Conf. on Acoust., Speech, and Signal Processing*, Philadelphia, USA, Mar. 2005.
- [14] S. Haykin, *Adaptive Filter Theory, 4rd ed.*, Englewood Cliffs, NJ: Prentice-Hall, 1996.
- [15] R. C. de Lamare and R. Sampaio-Neto, "Blind adaptive code-constrained constant modulus algorithms for CDMA interference suppression in multipath channels," *IEEE Communications Letters*, vol. 9, pp. 334-336, Apr. 2005.
- [16] Y. Chen, T. Le-Ngoc, B. Champagne, and C. Xu, "Recursive least squares constant modulus algorithm for blind adaptive array," *IEEE Trans. Signal Processing*, vol. 52, pp. 1452-1456, May 2004.
- [17] L. Wang, R. C. de Lamare, Y. Long Cai, "Low-complexity adaptive step size constrained constant modulus SG algorithms for adaptive beamforming", *Signal processing*, vol. 89, no. 12, 2503-2513.
- [18] A. M. Haimovich and Y. Bar-Ness, "An eigenanalysis interference canceler," *IEEE Trans. Signal Processing*, vol. 39, pp. 76-84, Jan. 1991.
- [19] X. Wang and H. V. Poor, "Blind multiuser detection: A subspace approach," *IEEE Trans. Information Theory*, vol. 44, pp. 677-690, Mar. 1998.
- [20] K. A. Byerly and R. A. Roberts, "Output power based partial adaptive array design," in *Twenty-Third Asilomar Conference on Signals, Systems, and Computers*, Pacific Grove, CA, pp. 576-580, Oct. 1989.
- [21] J. S. Goldstein and I. S. Reed, "Reduced-rank adaptive filtering," *IEEE Trans. Signal Processing*, vol. 45, pp. 492-496, Feb. 1997.
- [22] J. S. Goldstein and I. S. Reed, "Subspace selection for partially adaptive sensor array processing," *IEEE Trans. Aerospace and Electronic Systems*, vol. 33, pp. 539-544, Apr. 1997.
- [23] H. Ge, I. P. Kisteins, and L. L. Scharf, "Data dimensionality reduction using krylov subspaces: Making adaptive beamformer robust to model order-determination," *IEEE Proc. ICASSP 2006*, vol. 4, 14-19 May 2006.
- [24] L. L. Scharf, E. K. P. Chong, M. D. Zoltowski, J. S. Goldstein, and I. S. Reed, "Subspace expansion and the equivalence of conjugate direction and multistage Wiener filters," *IEEE Trans. Signal Processing*, vol. 56, pp. 5013-5019, Oct. 2008.
- [25] L. Wang and R. C. de Lamare, "Constrained adaptive filtering algorithms based on conjugate gradient techniques for beamforming", *IET Signal Processing*, vol. 4, no. 6, 686-697.
- [26] J. S. Goldstein, I. S. Reed, and L. L. Scharf, "A multistage representation of the Wiener filter based on orthogonal projections," *IEEE Trans. Information Theory*, vol. 44, pp. 2943-2959, Nov. 1998.
- [27] M. L. Honig and J. S. Goldstein, "Adaptive reduced-rank interference suppression based on the multistage Wiener filter," *IEEE Trans. Communications*, vol. 50, pp. 986-994, June 2002.
- [28] R. C. de Lamare, M. Haardt, and R. Sampaio-Neto, "Blind adaptive constrained reduced-rank parameter estimation based on constant modulus design for CDMA interference suppression," *IEEE Trans. Signal Proc.*, vol. 56, pp. 2470-2482, Jun. 2008.
- [29] W. Chen, U. Mitra, and P. Schniter, "On the equivalence of three reduced rank linear estimators with applications to DS-CDMA," *IEEE Trans. Information Theory*, vol. 48, pp. 2609-2614, Sep. 2002.
- [30] S. Burykh and K. Abed-Meraim, "Reduced-rank adaptive filtering using krylov subspace," *EURASIP Journal Applied Signal Processing*, pp. 1387-1400, Dec. 2002.
- [31] D. A. Pados and S. N. Batalama, "Joint space-time auxiliary-vector filtering for DS/CDMA systems with antenna arrays," *IEEE Trans. Commun.*, vol. 47, pp. 1406-1415, Sep. 1999.
- [32] D. A. Pados and G. N. Karystinos, "An iterative algorithm for the computation of the MVDR filter," *IEEE Trans. Signal Processing*, vol. 49, pp. 290-300, Feb. 2001.
- [33] R. C. de Lamare and R. Sampaio-Neto, "Adaptive Reduced-Rank MMSE Filtering with Interpolated FIR Filters and Adaptive Interpolators", *IEEE Sig. Proc. Letters*, vol. 12, no. 3, March, 2005.
- [34] R. C. de Lamare and Raimundo Sampaio-Neto, "Reduced-rank Interference Suppression for DS-CDMA based on Interpolated FIR Filters", *IEEE Communications Letters*, vol. 9, no. 3, March 2005.
- [35] R. C. de Lamare and R. Sampaio-Neto, "Adaptive Interference Suppression for DS-CDMA Systems based on Interpolated FIR Filters with Adaptive Interpolators in Multipath Channels", *IEEE Transactions on Vehicular Technology*, Vol. 56, no. 6, September 2007.
- [36] R. C. de Lamare and R. Sampaio-Neto, "Reduced-Rank Adaptive Filtering Based on Joint Iterative Optimization of Adaptive Filters", *IEEE Sig. Proc. Letters*, Vol. 14, no. 12, December 2007.
- [37] R. C. de Lamare, "Adaptive reduced-rank LCMV beamforming algorithms based on joint iterative optimization of filters," *Electronics Letters*, vol. 44, no. 9, Apr. 2008.
- [38] R. C. de Lamare and R. Sampaio-Neto, "Reduced-Rank Space-Time Adaptive Interference Suppression With Joint Iterative Least Squares Algorithms for Spread-Spectrum Systems," *IEEE Transactions on Vehicular Technology*, vol.59, no.3, March 2010, pp.1217-1228.
- [39] R. C. de Lamare and R. Sampaio-Neto, "Adaptive Reduced-Rank MMSE Parameter Estimation based on an Adaptive Diversity Combined Decimation and Interpolation Scheme," *Proc. IEEE International Conference on Acoustics, Speech and Signal Processing*, April 15-20, 2007, vol. 3, pp. III-1317-III-1320.
- [40] R. C. de Lamare and R. Sampaio-Neto, "Adaptive Reduced-Rank Processing Based on Joint and Iterative Interpolation, Decimation, and Filtering," *IEEE Transactions on Signal Processing*, vol. 57, no. 7, July 2009, pp. 2503 - 2514.
- [41] R.C. de Lamare, R. Sampaio-Neto, M. Haardt, "Blind Adaptive Constrained Constant-Modulus Reduced-Rank Interference Suppression Algorithms Based on Interpolation and Switched Decimation," *IEEE Transactions on Signal Processing*, vol.59, no.2, pp.681-695, Feb. 2011.
- R. C. de Lamare and R. Sampaio-Neto, "Adaptive reduced-rank equalization algorithms based on alternating optimization design techniques for MIMO systems," *IEEE Trans. Veh. Technol.*, vol. 60, no. 6, pp. 2482-2494, Jul. 2011.
- [42] M. J. Rude and L. J. Griffiths, "Incorporation of linear constraints into the constant modulus algorithm," *Acoustics, Speech, and Signal Processing, 1989. ICASSP-89., 1989 International Conference on*, vol. 2, pp. 968-971, May 1989.

- [43] V. Nagesha and S. Kay, "On frequency estimation with IQML algorithm," *IEEE Trans. Signal Processing*, vol. 42, pp. 2509- 2513, Sep. 1994.
- [44] J. S. Goldstein and I. S. Reed, "Theory of partially adaptive radar," *IEEE Trans. Aerospace and Electronic Systems*, vol. 33, pp. 1309-1325, Oct. 1997.
- [45] J. R. Guerci, J. S. Goldstein, and I. S. Reed, "Optimal and adaptive reduced-rank STAP," *IEEE Trans. Aerospace and Electronic Systems*, vol. 36, pp. 647-663, Apr. 2000.
- [46] R. Y. M. Wong and R. Adve, "Reduced-Rank Adaptive Filtering Using Localized Processing for CDMA Systems," *IEEE Trans. Vehicular Technology*, vol. 56, pp. 3846-3856, Nov. 2007.
- [47] S. J. Chern, C. H. Sun, and C. C. Chang, "Blind adaptive DS-CDMA receivers with sliding window constant modulus GSC-RLS algorithm," *Intelligent Signal Processing and Communication System, 2006, ISPACS-06., 2006 International Conference on*, pp. 979-982, Dec. 2006.
- [48] S. J. Chern and C. Y. Chang, "Adaptive MC-CDMA receiver with constrained constant modulus IQRD-RLS algorithm for MAI suppression," *Signal Processing*, vol. 83, pp. 2209-2226, Oct. 2003.
- [49] G. H. Golub and C. F. Van Loan, *Matrix Computations*, 3rd ed. Baltimore, MD: Johns Hopkins Univ. Press, 1996.
- [50] H. Qian and S. N. Batalama, "Data record-based criteria for the selection of an auxiliary vector estimator of the MMSE/MVDR filter," *IEEE Trans. Communications*, vol. 51, pp. 1700-1708, Oct. 2003.
- [51] C. J. Xu, G. Z. Feng, and K. S. Kwak, "A modified constrained constant modulus approach to blind adaptive multiuser detection," *IEEE Trans. Communications*, vol. 49, pp. 1642-1648, Sep. 2001.
- [52] D. P. Bertsekas, *Nonlinear Programming*, Athena Scientific, 2nd Ed., 1999.
- [53] P. Roger, "A generalized inverse for matrices", *Proceedings of the Cambridge Philosophical Society*, vol. 51, pp. 406-413, 1955.